

See discussions, stats, and author profiles for this publication at: <https://www.researchgate.net/publication/264634898>

Salt Stress-Induced Alterations in the Root Proteome of Amaranthus cruentus L.

ARTICLE *in* JOURNAL OF PROTEOME RESEARCH · JUNE 2014

Impact Factor: 4.25 · DOI: 10.1021/pr500153m · Source: PubMed

CITATIONS

5

READS

107

6 AUTHORS, INCLUDING:



José Ángel Huerta-Ocampo

Research Center for Food and Development A.C.

13 PUBLICATIONS 83 CITATIONS

[SEE PROFILE](#)



Alberto Barrera-Pacheco

Instituto Potosino de Investigación Científica ...

14 PUBLICATIONS 129 CITATIONS

[SEE PROFILE](#)



Eduardo Espitia Rangel

INIFAP Instituto Nacional de Investigaciones F...

56 PUBLICATIONS 60 CITATIONS

[SEE PROFILE](#)



Hans-Peter Mock

Leibniz Institute of Plant Genetics and Crop Pl...

124 PUBLICATIONS 4,391 CITATIONS

[SEE PROFILE](#)

Salt Stress-Induced Alterations in the Root Proteome of *Amaranthus cruentus* L.

José A. Huerta-Ocampo,[†] Alberto Barrera-Pacheco,[†] Christian S. Mendoza-Hernández,[†] Eduardo Espitia-Rangel,[‡] Hans-Peter Mock,[§] and Ana P. Barba de la Rosa^{*,†}

[†]IPICyT, Instituto Potosino de Investigación Científica y Tecnológica A.C., Camino a la Presa San José No. 2055, Lomas 4a Sección, 78216 San Luis Potosí, S.L.P., México

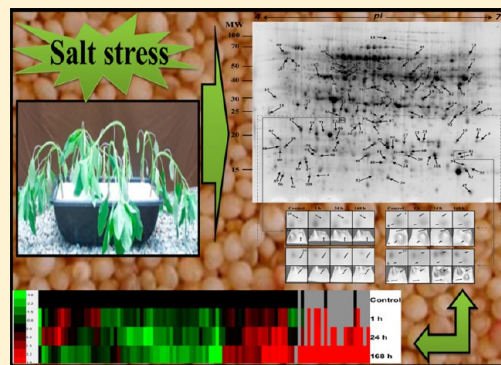
[‡]CIR, Centro de Investigación Regional del Centro-Instituto Nacional de Investigaciones Forestales, Agrícolas y Pecuarias. Km 13.5 de la Carretera los Reyes-Texcoco, Coatlinchan, Texcoco, Estado de México 56250, México

[§]Leibniz Institute of Plant Genetics and Crop Plant Research, Corrensstrasse 3, 06466 Gatersleben, Germany

Supporting Information

ABSTRACT: Salt stress is one of the major factors limiting crop productivity worldwide. Amaranth is a highly nutritious pseudocereal with remarkable nutraceutical properties; it is also a stress-tolerant plant, making it an alternative crop for sustainable food production in semiarid conditions. A two-dimensional electrophoresis gel coupled with a liquid chromatography–mass spectrometry/mass spectrometry (LC-MS/MS) approach was applied in order to analyze the changes in amaranth root protein accumulation in plants subjected to salt stress under hydroponic conditions during the osmotic phase (1 h), after recovery (24 h), and during the ionic phase of salt stress (168 h). A total of 101 protein spots were differentially accumulated in response to stress, in which 77 were successfully identified by LC-MS/MS and a database search against public and amaranth transcriptome databases. The resulting proteins were grouped into different categories of biological processes according to Gene Ontology. The identification of several protein isoforms with a change in pI and/or molecular weight reveals the importance of the salt-stress-induced posttranslational modifications in stress tolerance. Interestingly stress-responsive proteins unique to amaranth, for example, Ah24, were identified. Amaranth is a stress-tolerant alternative crop for sustainable food production, and the understanding of amaranth's stress tolerance mechanisms will provide valuable input to improve stress tolerance of other crop plants.

KEYWORDS: *Amaranthus cruentus* L., proteomics, roots, salinity



INTRODUCTION

Salt stress is one of the major abiotic stress factors that adversely affects crop productivity. High concentrations of salts in soils account for large decreases in the yield of a wide variety of crops.¹ It is expected that increased salinization of arable lands will have devastating global effects, rendering useless for crop production around 30% of agricultural lands within the next 25 years, and up to 50% by the year 2050.² Elevated levels of salt ions in soil solution surrounding plant roots induce an imbalance in water potential between plant root cells and ambient soil solution resulting in cellular dehydration. In addition, elevated salts lead to a passive salt ion penetration via plasma membrane and to an accumulation of salt ions in cell cytoplasm, which can lead to inhibition of intracellular enzyme activity.³ Exposure of plants to salt and other abiotic stress factors activates various physiological and developmental changes regulated by the expression of different genes and accumulation of their translated proteins activating diverse physiological, metabolic, and defense systems to survive.⁴

In crop plants, extensive efforts have been devoted to the generation of stress-tolerant genotypes by conventional breeding, but more frequently, conventional breeding has moved toward the exploitation of transgenics. The more frequent use of “omics” technologies has allowed the identification of genes and proteins associated with abiotic stress tolerance.⁵ Proteomic analysis has become one of the best strategies to reveal the dynamics of protein accumulation under salt stress.⁶ Several proteomic investigations have provided a new comprehension of plant root response and adaptation against salt stress. Proteins involved in stress signal perception including plasma membrane and cytoplasm receptors, G protein, calcium signaling and binding proteins, and phosphoproteins involved in kinase cascade activation have been found to be increased in abundance at the early stages of salt stress.⁷ As adaptive responses of plant roots to salt stress,

Received: February 18, 2014

Published: June 19, 2014

several molecular and cellular mechanisms carried out by proteins are triggered (e.g., modulation of the electrochemical gradient across the plasma membrane, alteration in carbohydrate and energy metabolism, modulation of ion channels to reduce cell dehydration and maintain ion homeostasis, as well as reactive oxygen species scavenging). In addition, changes in cytoskeleton organization and cell wall components are necessary in order to adjust cell size and maintain cell turgor.⁸

The genus *Amaranthus* belongs to the order of *Caryophyllales* and to the family *Amaranthaceae* that includes about 70 genera and 800 species of herbs of tropical origin that have evolved in warm regions as well as in dry and saline soils, leading to physiological adaptations to cope with these harsh environments.⁹ Amaranth (*Amaranthus* spp.) is a promising vegetable species often grown under semiarid conditions prone to both drought and salinity.¹⁰ Some of the amaranth species are known as weeds, whereas the grain amaranth species (*A. cruentus*, *A. caudatus*, and *A. hypochondriacus*) are recognized by their high nutritional value. Amaranth seeds contain around 15 to 17% protein, containing an amino acid composition close to the optimal balance required for human diet, being rich in essential amino acids such as lysine and methionine.¹¹ Amaranth leaves have a high content of minerals such as calcium, iron, magnesium, and phosphorus, plus vitamins A and C.¹² Due to the high quality of amaranth proteins, crops such as corn, wheat, and potatoes have been genetically transformed with amaranth seed storage proteins in order to increase the nutritional value and content of essential amino acids in these crops.^{13–15} In addition to its recognized stress tolerance and high nutritional values, amaranth is a nonallergenic food with remarkable nutraceutical properties.¹⁶

The increased ability to withstand drought stress and the high salt tolerance of grain amaranth has been associated with a high water-use efficiency.¹⁷ Genetic information underlying the mechanisms that confer to amaranth its capacity to withstand drought and/or salt stress is limited, although several abiotic stress related genes have been identified in amaranth and in genetically related species such as spinach, cultivated and wild species of beet root, *Mesembryanthemum crystallinum*, and the halophytes *Suaeda* spp., *Salicornia* spp., and *Atriplex* spp.¹⁸

To date, there are no reports on the analysis of proteins involved in the response to NaCl stress in amaranth roots. Previous works using a combined proteomic/subtractive hybridization approach suggested that amaranth's root response to drought stress involves a coordinated response that includes osmolyte accumulation and the activation of stress-related genes needed for the scavenging of reactive oxygen species, protein stabilization, and transcriptional regulation of plant growth.¹⁹ Because roots are the primary sites of stress perception, the aim of this work was to identify differentially accumulated proteins in *A. cruentus* L. roots subjected to mild-moderate salt stress with 150 mM NaCl under hydroponic conditions. Such NaCl concentration was chosen in order to avoid the evaluation of changes reflecting the cellular damage caused by severe stress that may mask more important responsive proteins related with the molecular and physiological responses that allow amaranth to tolerate salt-stress conditions.

Identification of calcium-stress-induced genes in amaranth leaves through suppression subtractive hybridization has also contributed to increase the relatively low number of grain amaranth expressed sequence tags (ESTs) responsive to abiotic stress conditions.²⁰ The utilization of 454 pyrosequencing

technology was employed as a tool to obtain genomic data from *Amaranthus tuberculatus*, a notorious weed of maize and soybean crops in the United States,²¹ and notably the publication of the first large-scale transcriptomic analysis of nonweed amaranth where different sources of RNA (plants subjected to drought and acute salt stress among other conditions) were used to generate the cDNA libraries.¹⁸ These libraries gives the tools for a reliable identification of more amaranth stress-responsive proteins using the proteomic approach and surely will contribute to the elucidation of the salt-stress-tolerance mechanisms in amaranth.

EXPERIMENTAL PROCEDURES

Plant Materials, Salt Stress Treatment, and Plant Harvest

Amaranth seeds (*Amaranthus cruentus* L. cv. Amaranteca) were obtained from the National Institute for Investigation in Forestry, Agriculture and Animal Production (INIFAP, Mexico). Seeds were germinated on soil for horticulture (Peat Moss Tourbe, Premier Horticulture, Québec, Canada). After germination, clean seedlings were transferred to plastic trays (60 × 45 × 15 cm) that were filled with 1/2 strength nutrient solution (Hydro-Environment, México) with an electrical conductivity (EC) of 2.0–2.2 ds m⁻¹ and renewed every week. Trays were placed in a greenhouse under 30/25 °C day/night temperature and a photoperiod of 12 h light/12 h dark. After preculture of amaranth seedlings for one month, 150 mM NaCl were added to the nutrient solution (EC 16.9–17.2 ds m⁻¹). Samples were collected after 1, 24, and 168 h after salt-stress imposition. Biological replicates were independently carried out three times, and plants were harvested, pooled, and used for the experiments separately.

Total Soluble Sugar and Free Proline Contents

Free proline and total soluble sugar contents were determined in roots of plants subjected to progressive salt stress. Free proline was determined using the ninhydrin reaction according to Magne and Larher.²² Samples were milled, and proline was extracted by boiling 0.5 g of powdered roots in 2 mL of water. Then, 0.5 mL of sodium citrate (0.2 M pH 4.6) and 2 mL of 1% ninhydrin in (acetic acid/water, 60:40) solution were added to 0.5 mL of the resulting extract. Mixture was incubated in boiling water for 1 h. The reaction mixture was extracted with 2 mL of toluene and proline concentration was calculated on the basis of absorbance of the resulting chromophore at 520 nm in a spectrophotometer (8453 UV-visible Spectrophotometer, Agilent Technologies, Santa Clara, CA, U.S.A.) using toluene as blank and L-proline (Sigma-Aldrich, St Louis, MO, U.S.A.) as standard. Three technical replicates for each of three biological replicates were analyzed.

Total soluble sugar in ethanol was determined using anthrone as reported by Aghaei et al.²³ Roots (500 mg) were crushed in 5 mL of ethanol; the insoluble fraction was washed with 70% ethanol. Alcohol soluble fractions were centrifuged at 3500g for 10 min. The supernatants were collected, and 3 mL of freshly prepared anthrone reagent (150 mg of anthrone in 100 mL of 72% H₂SO₄) was added to 0.1 mL of the alcoholic extract. The mixture was placed for 10 min in a boiling water bath, and the reaction was stopped after the tube was transferred to an ice bath. After cooling, the absorbance was measured at 625 nm using a spectrophotometer. D-Glucose (Invitrogen, Carlsbad, CA, U.S.A.) was used as standard. Three technical replicates for each of three biological replicates were analyzed.

Ion Content Analysis

Prior to determination of ion content, the seedlings were uprooted and washed with deionized water. Leaves and roots samples were dried in an 80 °C oven until constant weight was reached. Dried materials were ashed in a furnace for 4 h at 500 °C, ashes were dissolved with 1.0 N HCl solution and diluted in deionized water into a volumetric flask. The contents of Na⁺ and K⁺ in roots were determined using an atomic absorption spectrometer (AAAnalyst 400, PerkinElmer, Waltham MA, U.S.A.). Three technical replicates for each of three biological replicates were analyzed.

Protein Sample Preparation

Root samples were frozen in liquid nitrogen and milled in a coffee grinder (Braun, Naucalpan, Mexico) to a fine powder and suspended in extraction buffer (40 mM Tris pH 8.0, 1% polyvinylpolypyrrolidone and 2% phenylmethylsulfonyl fluoride). The mixture was sonicated (GE-505, Ultrasonic Processor, Sonics & Materials, Inc., Newtown, CT, U.S.A.) for 15 min at 4 °C and centrifuged for 10 min at 10 000g (Super T21; Sorvall, Kendro Laboratory Products, Newtown, CT, U.S.A.). The supernatant was filtered with Miracloth (Calbiochem, Darmstadt, Germany) and treated with Nuclease Mix (GE Healthcare, Piscataway, NJ, U.S.A.) according to manufacturer's instructions, mixed with three parts of cold acetone containing 10% trichloroacetic acid and 2% 2-mercaptoethanol, and incubated overnight at -20 °C. After 30 min of centrifugation at 13 000g, the protein pellet was recovered and washed once in cold methanol and three times in cold acetone. The resulting pellet was dried and suspended in rehydration buffer [8 M urea, 2% 3-[3-cholamidopropyl]-dimethylammonio]-1-propanesulfonate, 0.56% dithiothreitol, 0.002% bromophenol blue] and 0.5% IPG buffer pH 4–7 (Bio-Rad, Hercules, CA, U.S.A.). Protein concentration was determined using the RC/DC Protein Assay (Bio-Rad) with BSA as standard. Root proteins were extracted from three independent biological replicates.

Two-Dimensional Electrophoresis (2-DE) and Image Analysis

Isoelectric focusing (IEF) was carried out onto 24 cm IPG linear gradient strips of pH 4–7 (Bio-Rad). Strips were rehydrated with 0.5 and 1.5 mg of total protein for analytical and preparative gels, respectively. Focusing was conducted at 20 °C with an Ettan IPGphor system (GE Healthcare) at constant 50 mA per strip under the following conditions: (I) 500 V gradient until 0.01 kWh, (II) 4000 V gradient until 5.6 kWh, and (III) holding at 8000 V until 60 kWh. After IEF, the IPG strips were stored at -20 °C or immediately equilibrated twice for 15 min in equilibration buffer (6 M urea, 30% glycerol, 2% SDS, 50 mM Tris-HCl buffer pH 8.8), the first time containing 1% dithiothreitol and the second time equilibration was performed in the same solution now containing 2.5% iodoacetamide instead of dithiothreitol. The strips were placed directly onto 13% polyacrylamide-SDS slab gels. The separation was conducted using the Ettan Daltix Electrophoresis unit (GE Healthcare). Preparative gels were stained with PhastGel Blue R (GE Healthcare). Analytical gels were stained with SyproRuby Protein Gel Stain (Molecular Probes, Eugene, OR, U.S.A.) and scanned at 100 μm resolution with Pharos FX Plus Molecular Imager (Bio-Rad). Image analysis was performed with PDQuest 2-D Analysis Software v8.0 (Bio-Rad). Experimental molecular mass of each protein spot was estimated by comparison with molecular weight

standards (BenchMark Protein Ladder, Invitrogen). Experimental pI was determined by migration of protein spots on the IPG linear gradient strips. Protein spots were considered as differentially accumulated when their normalized volumes displayed a fold change ≥2 when controls and treatments were compared. Significant changes were determined using *t*-test (*P* < 0.05).

In-Gel Digestion and Tandem Mass Spectrometry Analysis (LC-MS/MS)

Differentially accumulated protein spots were excised from the preparative gels and destained; they were reduced with 10 mM dithiothreitol in 25 mM ammonium bicarbonate, followed by protein alkylation with 55 mM iodoacetamide. Protein digestion was carried out overnight at 37 °C with sequencing-grade trypsin (Promega, Madison, WI, U.S.A.). Nanoscale LC separation of tryptic peptides was performed with a nanoACQUITY UPLC System (Waters, Milford, MA, U.S.A.) equipped with a Symmetry C₁₈ precolumn (5 μm, 20 mm × 180 μm, Waters) and a BEH130 C₁₈ (1.7 μm, 100 mm × 100 μm, Waters) analytical column. The lock mass compound, [Glu¹]-Fibrinopeptide B (Sigma-Aldrich), was delivered by the auxiliary pump of the nanoACQUITY UPLC System at 200 nL/min at a concentration of 100 fmol/mL to the reference sprayer of the Nano-Lock-Spray source of the mass spectrometer. Mass spectrometric analysis (LC-MS/MS) was carried out in a SYNAPT-HDMS Q-TOF (Waters). The spectrometer was operated in V-mode, and analyses were performed in positive mode ESI. The TOF analyzer was externally calibrated with [Glu¹]-Fibrinopeptide B from *m/z* 50 to 2422. The data were lock-mass corrected postacquisition using the doubly protonated monoisotopic ion of [Glu¹]-Fibrinopeptide B. The reference sprayer was sampled every 30 s. The RF applied to the quadrupole was adjusted such that ions from *m/z* 50–2000 were efficiently transmitted. MS and MS/MS spectra were acquired alternating between low-energy and elevated-energy mode of acquisition (MS^e).

Protein Identification Using MS/MS Data Sets and Database Searching

MS/MS spectra data sets were used to generate PKL files using Protein Lynx Global Server v2.4 (PLGS, Waters). Proteins were then identified using PKL files and the MASCOT search engine v2.3 (Matrix Science, London, U.K.). Searches were conducted against the *Viridiplantae* subset of the NCBI protein database (1 622 297 sequences, December 2013) and against the *A. hypochondriacus* transcriptome database (127 242 sequences, December 2013). Trypsin was used as the specific protease, and one missed cleavage was allowed. The mass tolerance for precursor and fragment ions was set to 10 ppm and 0.05 Da, respectively. Carbamidomethyl cysteine was set as fixed modification and oxidation of methionine was specified as variable modification. The protein identification criteria included at least two MS/MS spectra matched at 99% level of confidence, and identifications were considered successful when significant MASCOT scores (>43 for the *Viridiplantae* subset of the NCBI protein database or >33 for *A. hypochondriacus* transcriptome database) were obtained, indicating the identity or extensive homology at *P* < 0.01 and the presence of a consecutive y ion series of more than three amino acids.

Protein Classification and Hierarchical Cluster Analysis

Hierarchical clustering of the protein spot accumulation profiles was performed on the log transformed spot abundance ratios at

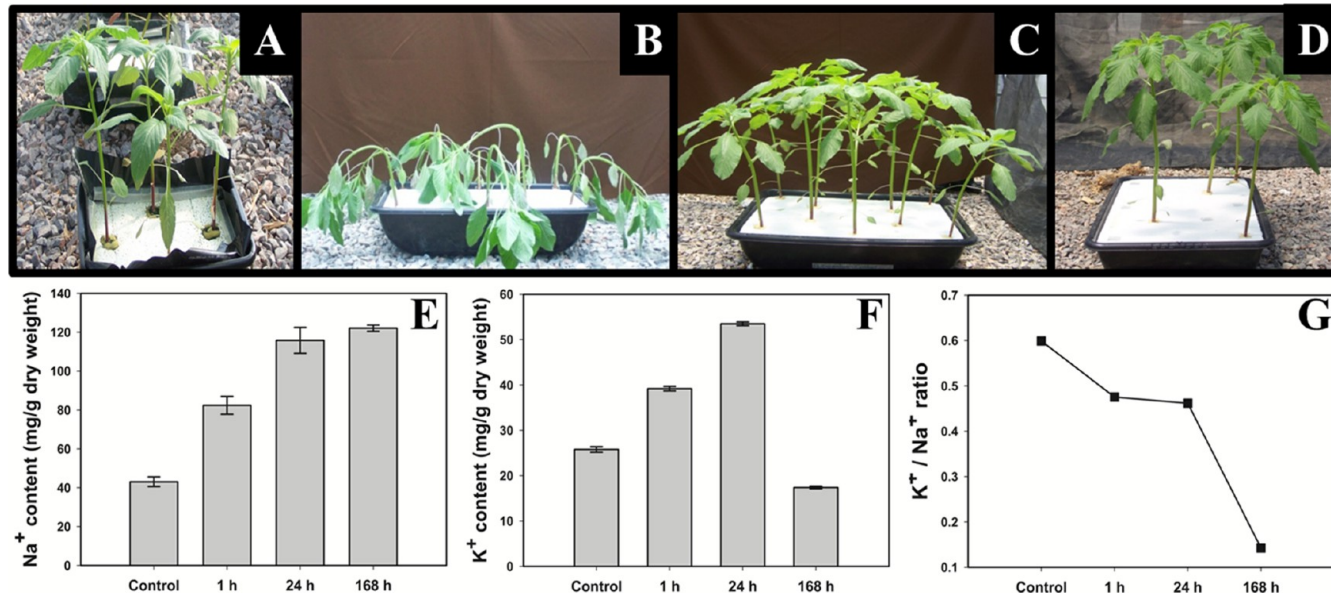


Figure 1. Salt stress-induced physiological changes in *Amaranthus cruentus* grown under hydroponic conditions. Plants were grown for 1 month in 1/2 strength nutrient solution (A) and then 150 mM NaCl was added to the nutrient solution. Root samples were collected after 1 h (B), 24 h (C), and 168 h (D) of salt-stress imposition. The effect of salt stress on Na⁺ content (E), K⁺ content (F), and K⁺/Na⁺ ratio (G) are presented. The values are presented as means \pm SE of three biological replicates analyzed by triplicate.

the different time points of stress compared to controls using the software Cluster v 3.0 (Available at <http://bonsai.hgc.jp/~mdehoon/software/cluster/index.html>). The program TreeView (<http://jtreeview.sourceforge.net/>) was used to generate the graphical view of the results obtained from Cluster v 3.0. Identified proteins were classified into different categories of biological processes in which they are involved according to Gene Ontology (<http://www.geneontology.org/>).

RESULTS AND DISCUSSION

Effect of Salt Stress on *A. cruentus* Cultivated under Hydroponic Conditions

For the proteomic analysis of the amaranth root response to salt stress, it was necessary to prepare plants of uniform size and cultured under stable growth conditions. In this study, amaranth plants (*A. cruentus* L. cv. Amaranteca) were grown under hydroponic conditions (Figure 1A). NaCl (150 mM) was added to the nutrient solution; therefore, amaranth roots were directly in contact with salt. This system allowed a reproducible and fast root tissue sampling. Two well-defined phases occur during salt stress: (1) the osmotic phase of rapid onset, when high concentrations of salts in the soil make it harder for roots to extract water and the resulting change in the osmotic pressure has an immediate effect on plant metabolism; and (2) the ion-specific phase that is due to the accumulation of Na⁺ in plant tissues (mainly leaves). In the ion-specific phase, salt accumulates to toxic concentrations in the older leaves which are no longer expanding and so no longer diluting the salt arriving to them as younger growing leaves do, and they die. If the rate at which they die is greater than the rate at which new leaves are produced, the photosynthetic capacity of the plant will no longer be able to supply the carbohydrate requirements of the young leaves, which further reduces their growth rate.²⁴

The osmotic phase in amaranth roots was observed after 1 h of salt addition (Figure 1B), and at this time, the salt

concentration around the roots increased to a threshold level; after 24 h, the amaranth plants were recovered from the osmotic phase of stress (Figure 1C), and finally after 168 h (Figure 1D), salt-stressed plants exhibited slight phenotypic differences in comparison with controls, such as slight curling of leaves and accelerated senescence of the older leaves, indicating the presence of the ionic phase of salt stress. Gene expression and accumulation of their translated proteins varies in relation to the time after the salt shock is applied. It is likely that many genes and their translated proteins induced soon after salt is applied are related to the response to the osmotic component of salt stress and can be more similar to that occurring during water or other osmotic stresses rather than those genes/proteins specifically responding to the ionic component of salt stress.

Changes in Ion Contents and Osmolytes

As a result of the treatment, Na⁺ content increased very fast (2-fold) after only 1 h, and after 24 h, Na⁺ content reached about 120 mg/g DW; however, after 168 h, there was no significant difference in the root Na⁺ content in comparison to that obtained after 24 h (Figure 1E). K⁺ content slightly increased after 1 h of salt-stress imposition, and after 24 h, its concentration was doubled; however, K⁺ content dramatically declined after 168 h (Figure 1F). The K⁺/Na⁺ ratios decreased gradually with the progression of salt-stress imposition (Figure 1G).

Na⁺ exclusion by leaf blades or by roots ensures that Na⁺ does not accumulate to toxic concentrations within leaves. A failure in Na⁺ exclusion manifests its toxic effect after days or weeks depending on the species and causes premature death of older leaves.²⁵ As far as we know, *A. cruentus* does not have such mechanisms; therefore, tolerance requires compartmentalization of Na⁺ at the cellular and intracellular level to avoid toxic concentrations within the cytoplasm, especially in mesophyll cells in the leaf. Toxicity occurs with time, after leaf Na⁺ increases to high concentrations in the older leaves.

Restoration of water relations typically requires the uptake of osmoticum in the form of Cl^- and Na^+ ions.²⁵ These are predominantly stored in the vacuole with a concomitant loss of cellular K^+ , and the disproportionate presence of Na^+ in cellular and extracellular compartments negatively impacts the acquisition of essential nutrients such as Ca^{2+} and K^{+} .²⁵

Synthesis of osmolytes is another important mechanism for tissue tolerance to salt stress, and in order to evaluate the effects of salt stress on the production of osmoprotective substances, free proline and soluble sugars contents were determined in roots of controls and in salt-stressed plants. After addition of 150 mM NaCl to the hydroponic nutritive solution, root free proline contents remain almost unchanged during the first 24 h, and a slight decrease after 1 h of stress imposition was observed. The maximum free proline contents were observed after 168 h of stress imposition and corresponded to a 3-fold increase (Figure 2A). Accumulation of free proline is a

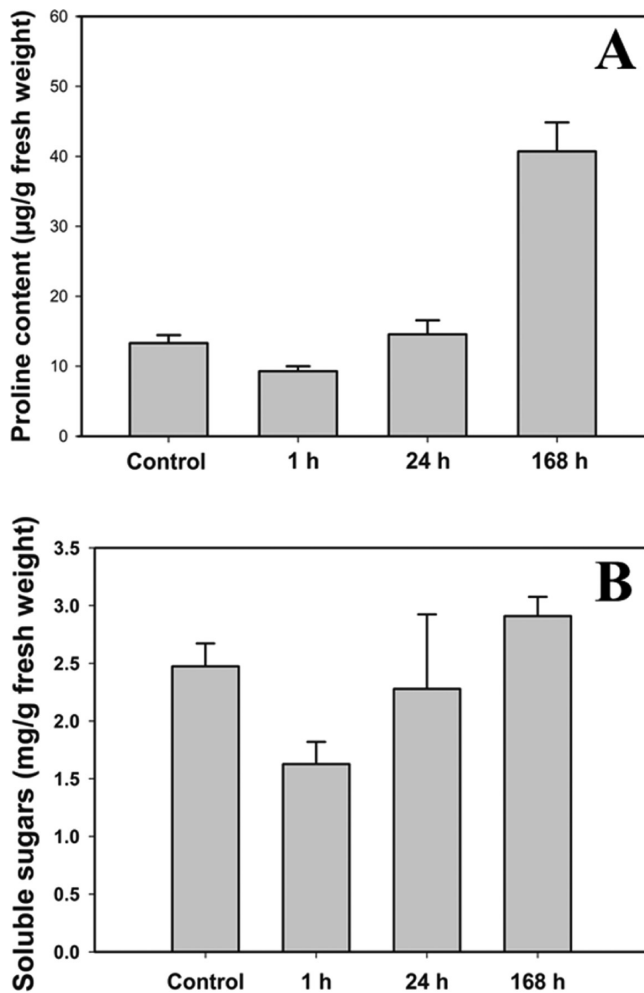


Figure 2. Effect of salt stress on free proline (A) and soluble sugar (B) contents in amaranth roots. The values are presented as means \pm SE of samples analyzed in triplicate.

common response to abiotic stresses; several studies suggest that proline is involved in the osmotic adjustment between the cytoplasm and vacuole. It has been also suggested that proline can act as a protective agent for enzymes, as a free-radical scavenger, or as a storage compound for carbon and nitrogen to allow recovery from stress.²³ The content of soluble sugars remained significantly unchanged after 24 and 168 h after salt-

stress imposition. A slight decrease was observed after 1 h under salt stress (Figure 2B). The role of soluble sugars in amaranth subjected to salt stress is not clear. Soluble sugar as osmoprotectants can counteract the ionic toxic effects in shoots of several species of plants under salt stress.²⁶

Identification of Salt Stress-Responsive Proteins by 2-DE and LC-MS/MS

In order to analyze the proteome changes in amaranth roots under salt stress in plants subjected to 150 mM NaCl, the 2-DE gel coupled with LC-MS/MS approach was applied. Roots were harvested, and proteins were extracted and separated by 2-DE. Out of more than 600 reproducibly detected protein spots, 101 spots showed significant and at least 2-fold changes in abundance in salt-stressed samples at least at one stage compared with control plants. Figure 3 shows the position of the 101 differentially accumulated protein spots on a 2-DE gel of root proteins from amaranth plants harvested after 168 h of salt stress imposition. A close-up and three-dimensional (3D) view of one spot that disappears after 168 h of salt stress imposition (spot 84) and other five differentially accumulated protein spots are also shown in Figure 3. The 2-DE gel images used for analysis and close-up views and graphical accumulation patterns of some of the differentially accumulated protein spots are shown in Supporting Information Figures S1 and S2.

The number of significantly increased protein spots in amaranth roots increased from 16 after 1 h to 33 after 24 h and up to 45 after 168 h of salt stress imposition. The significantly decreased protein spots were from 17 after 1 h to 27 after 24 h and up to 40 after 168 h of salt stress imposition (Supporting Information Figure S3). Protein spots were excised from preparative 2-DE gels and subsequently subjected to LC-MS/MS analysis. Seventy-seven spots were successfully identified ($P < 0.01$) by searching against the *Viridiplantae* subset of the NCBI nr and the *A. hypochondriacus* transcriptome databases, and in 13 cases, the same spot matched to more than one protein (Table 1, Supporting Information Table S1). 2-DE is still the most widely used method to resolve complex protein mixtures. It provides high resolution and enables identification of posttranslational modifications and proteolysis in a reference map format.²⁷ It is almost impossible to resolve an entire proteome in a 2-DE. Thus, even using a large format (24 cm IPG strips) and narrow pH range (4–7), it is not surprising that in this work many apparently well-resolved protein spots isolated from 2-DE gels matched and indeed contained more than a single protein. This observation may be a challenge for proper interpretation of the protein changes reported here; however, the criteria used for protein identification including a narrow tolerance for precursor and fragment ions as well as the minimum of two peptides and a high level of confidence (99%) support the identification of more than one protein in a protein spot; in most of these identifications, more than three peptides and very close theoretical and experimental molecular weight and isoelectric point values reinforce the presence of more than one protein in a single spot.

As shown in Figure 4, hierarchical clustering offered a global view of the differential accumulation patterns of protein spots. Spot cluster I consisted mainly of proteins absent in controls and during the first 1 and 24 h after stress imposition that appear only under stress conditions. Unfortunately, 9 of the 20 spots in this cluster were not identified, whereas the 11 identified spots are involved in different biological processes (Table 1). Cluster II involves spots clearly increased most

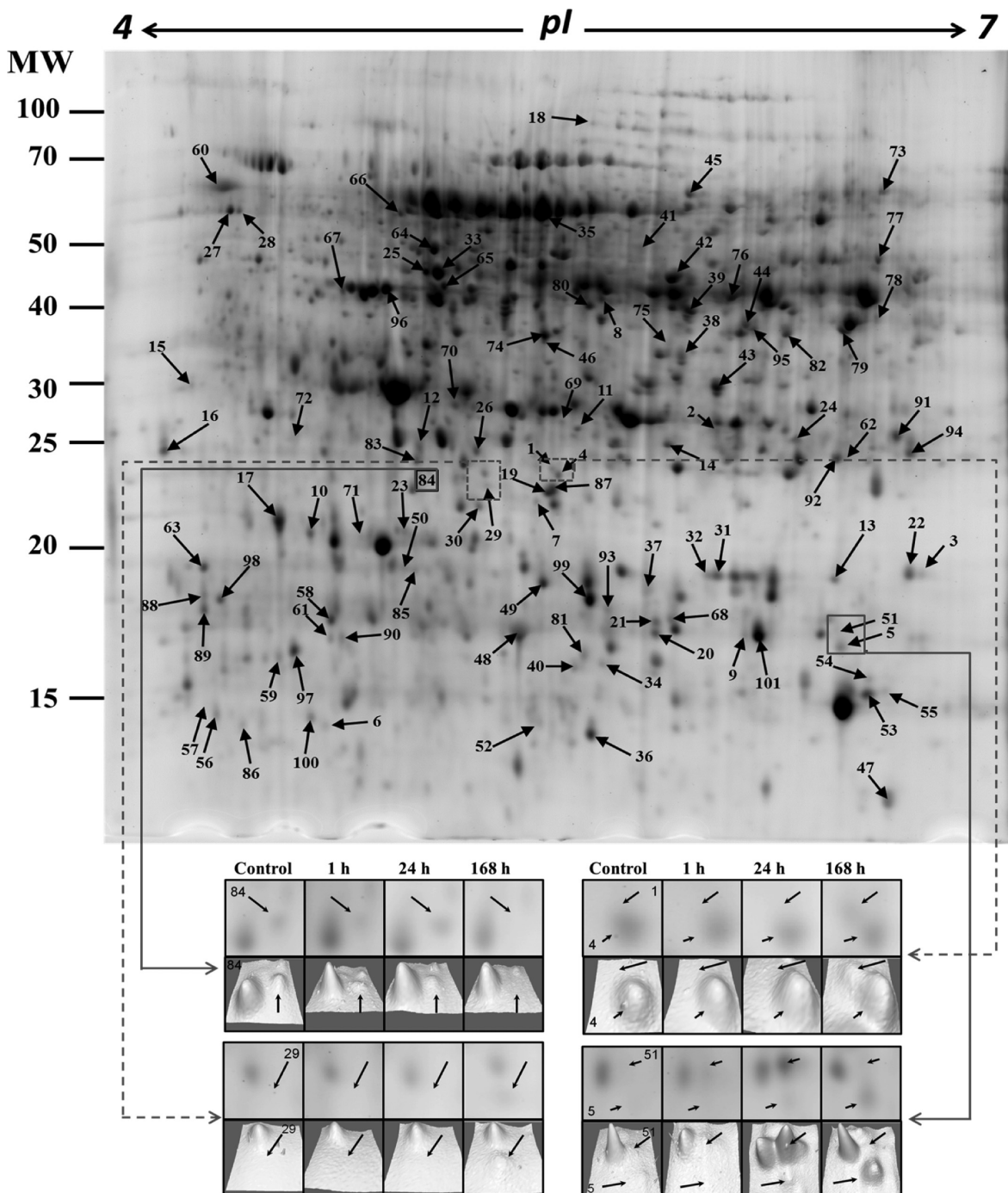


Figure 3. Sypro Ruby-stained 2-DE gel. Protein was extracted from roots of *Amaranthus cruentus* under 150 mM NaCl stress conditions for 7 days and separated on 24 cm IPG strips (pH 4–7 linear gradient) using IEF in the first dimension, followed by 13% SDS-PAGE in the second dimension. Spot numbers indicate the 101 analyzed spots including the 77 identified (64 spots with a single protein match 13 spots matched to more than one protein) and the 24 unidentified spots. For some spots, examples of changes in spot abundance including a 3D view among the analyzed conditions are presented.

considerably after 24 and 168 h after stress imposition, and most of the proteins identified in this cluster are involved in reactive oxygen species scavenging and detoxification. Spot cluster III included proteins decreased in abundance in response to salt stress, this cluster predominantly include proteins involved in carbohydrate metabolism and proteins related to physiological defense response; these spots mostly displayed decreased accumulation in response to salt stress. Spots in cluster IV showed high abundance in response to the

dramatic osmotic change induced after 1 h of salt stress imposition; these spots included proteins involved in protein folding and degradation. Finally, spots in cluster V were increased in response to the first 1 and 24 h of stress imposition. Proteins identified in these spots are related to diverse biological processes.

Interestingly, among the 77 identified protein spots, 3 amaranth root proteins (threonine synthase, spot 45; malate dehydrogenase, spot 65, and nucleoside diphosphate kinase 4,

Table 1. Identification of Differentially Accumulated Root Proteins in *Amaranthus cruentus* L. Plants Subjected to Salt Stress

Spot No. ^(a)	Protein	Plant species ^(b)	Accession number ^(c)	Exper. kDa/pI ^(d)	Theor. kDa/pI ^(e)	Mascot Score ^(f)	PM ^(g)	DB ^(h)	Ctrl ⁽ⁱ⁾	Fold change ^(j)			V%±SE ^(k)
										1 h	24 h	168 h	
ATP synthesis													
25	ATP synthase beta subunit 1	<i>Gossypium hirsutum</i>	gi 242129046	46.9/5.14	59.8/5.90	115	7	Ah	X	X	X	✓	
66	ATP synthase beta subunit 1	<i>Gossypium hirsutum</i>	gi 242129046	57.3/5.06	59.8/5.90	81	3	Ah	✓	0.43	0.73	0.60	
Carbohydrate metabolism													
8	Fructose-bisphosphate aldolase, cytoplasmic	<i>Spinacia oleracea</i>	gi 113624	42.1/5.74	38.4/5.96	584	18	Ah	✓	0.65	0.46	0.31	
(12)	Fructose-bisphosphate aldolase, cytoplasmic	<i>Spinacia oleracea</i>	gi 113624	24.7/5.12	38.4/5.96	188	3	Ah	✓	0.50	0.25	0.44	
(33)	Fructose-bisphosphate aldolase, cytoplasmic	<i>Spinacia oleracea</i>	gi 113624	46.6/5.18	38.4/5.96	36	3	Ah	✓	0.45	0.94	1.19	
(33)	Lactate/malate dehydrogenase family protein	<i>Theobroma cacao</i>	gi 508714144	46.6/5.18	35.7/6.60	34	3	Ah	✓	0.45	0.94	1.19	
35	Enolase	<i>Spinacia oleracea</i>	gi 8919731	57.5/5.49	48.1/5.49	783	20	Ah	✓	0.50	0.45	1.02	
(39)	Fructose-bisphosphate aldolase, cytoplasmic	<i>Spinacia oleracea</i>	gi 113624	40.0/6.00	38.4/5.96	430	12	Ah	✓	0.60	0.30	0.30	
(39)	Enolase	<i>Spinacia oleracea</i>	gi 8919731	40.0/6.00	48.1/5.49	79	4	Ah	✓	0.60	0.30	0.30	
(41)	Fructose-bisphosphate aldolase, cytoplasmic	<i>Spinacia oleracea</i>	gi 113624	50.8/5.86	38.4/5.96	491	15	Ah	✓	0.55	1.78	0.29	
42	Fructose-bisphosphate aldolase, cytoplasmic	<i>Spinacia oleracea</i>	gi 113624	45.5/5.95	38.4/5.96	147	9	Ah	✓	7.75	8.46	40.8	
44	Mitochondrial NAD-dependent malate dehydrogenase	<i>Solanum tuberosum</i>	gi 21388544	37.7/6.17	36.2/8.87	110	7	Ah	✓	0.55	0.44	0.20	
65	Malate dehydrogenase, chloroplastic-like	<i>Vitis vinifera</i>	gi 225452831	44.1/5.20	43.7/8.09	47	5	Ah	✓	0.48	0.67	0.64	
(67)	Fructokinase	<i>Beta vulgaris</i>	gi 1052973	43.3/4.88	35.4/5.38	58	9	Ah	✓	0.66	0.42	0.35	
(67)	Pyruvate dehydrogenase E1 component subunit beta	<i>Cucumis sativus</i>	gi 449445580	43.3/4.88	39.6/5.60	377	13	Ah	✓	0.66	0.42	0.35	
(70)	Triosephosphate isomerase	<i>Oryza sativa Japonica Group</i>	gi 306415973	27.8/5.24	27.0/5.38	61	5	Ah	✓	0.59	0.34	0.23	
75	Fructose-bisphosphate aldolase, cytoplasmic	<i>Spinacia oleracea</i>	gi 113624	35.3/5.94	38.4/5.96	433	14	Ah	✓	0.27	0.11	0.05	
76	Lactate/malate dehydrogenase family protein	<i>Theobroma cacao</i>	gi 508714144	42.3/6.13	35.7/6.60	303	12	Ah	✓	1.15	0.71	0.43	
79	Malate dehydrogenase, mitochondrial-like	<i>Glycine max</i>	gi 356517066	37.0/6.46	36.0/8.22	342	9	Ah	✓	1.07	2.00	0.84	

Table 1. continued

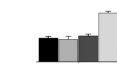
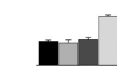
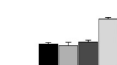
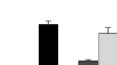
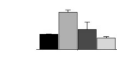
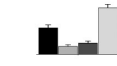
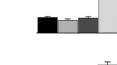
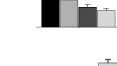
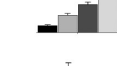
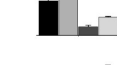
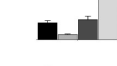
Spot No. ^(a)	Protein	Plant species ^(b)	Accession number ^(c)	Exper. kDa/pI ^(d)	Theor. kDa/pI ^(e)	Mascot Score ^(f)	PM ^(g)	DB ^(h)	Ctrl ⁽ⁱ⁾	Fold change ^(j)			V%±SE ^(k) Control 1 h 24 h 168 h
										1 h	24 h	168 h	
(80)	Fructose-bisphosphate aldolase, cytoplasmic	<i>Spinacia oleracea</i>	gi 113624	40.9/5.70	38.4/5.96	239	13	Ah	✓	0.94	1.09	2.06	
(80)	Enolase	<i>Spinacia oleracea</i>	gi 8919731	40.9/5.70	48.1/5.49	75	6	Ah	✓	0.94	1.09	2.06	
(80)	Lactate/malate dehydrogenase family protein	<i>Theobroma cacao</i>	gi 508714144	40.9/5.70	35.7/6.60	73	5	Ah	✓	0.94	1.09	2.06	
82	Fructose-bisphosphate aldolase, cytoplasmic	<i>Spinacia oleracea</i>	gi 113624	36.3/6.29	38.4/5.96	55	2	Ah	✓	0.10	0.22	0.81	
95	Mitochondrial NAD-dependent malate dehydrogenase	<i>Solanum tuberosum</i>	gi 21388544	37.1/6.19	36.2/8.87	136	5	Ah	X	X	X	✓	
96	Fructokinase	<i>Beta vulgaris</i>	gi 1052973	43.6/5.01	35.4/5.38	236	12	Ah	X	X	X	✓	
Protein folding													
3	Peptidyl-prolyl cis-trans isomerase CYP20-2	<i>Vitis vinifera</i>	gi 359473789	19.2/6.67	28.0/9.65	299	7	Ah	✓	2.46	1.33	0.75	
22	Peptidyl-prolyl cis-trans isomerase CYP20-2	<i>Vitis vinifera</i>	gi 359473789	19.2/6.64	28.0/9.65	122	5	Ah	✓	0.30	0.42	1.77	
60	Calreticulin	<i>Beta vulgaris</i>	gi 11131631	59.5/4.48	48.1/4.95	291	17	Ah	✓	1.78	1.09	0.39	
Nucleotide metabolism													
7	dUTP pyrophosphatase	<i>Arabidopsis thaliana</i>	gi 15232681	22.2/5.47	17.5/5.34	51	2	Ah	X	X	✓	✓	
(53)	Nucleoside diphosphate kinase I	<i>Mesembryanthemum crystallinum</i>	gi 6225750	14.9/6.54	16.3/6.30	54	4	Ah	✓	0.84	0.99	3.09	
68	Nucleoside diphosphate kinase 4, chloroplastic	<i>Spinacia oleracea</i>	gi 45477151	17.5/5.95	25.7/9.15	79	10	Ah	X	X	✓	✓	
Cell redox homeostasis													
(4)	Dehydroascorbate reductase	<i>Nicotiana tabacum</i>	gi 28192427	23.4/5.54	23.7/7.70	234	9	Ah	✓	0.64	0.46	0.39	
14	Dehydroascorbate reductase	<i>Nicotiana tabacum</i>	gi 28192427	24.9/5.94	23.7/7.70	244	6	Ah	✓	2.58	4.16	6.79	
18	NADH-ubiquinone oxidoreductase	<i>Ricinus communis</i>	gi 255582280	82.7/5.72	80.7/6.56	94	4	NCBI	✓	1.21	0.25	0.53	
(45)	Monodehydroascorbate reductase	<i>Spinacia oleracea</i>	gi 15320419	59.0/6.00	54.0/6.65	111	16	Ah	✓	0.30	1.19	2.89	
52	Thioredoxin h	<i>Olea europaea</i>	gi 399605022	14.1/5.46	13.5/5.91	152	4	Ah	✓	0.37	0.87	0.33	
73	Dihydrolipoyl dehydrogenase, mitochondrial-like	<i>Glycine max</i>	gi 356565179	59.8/6.57	52.8/6.90	316	19	Ah	✓	0.70	0.17	0.56	

Table 1. continued

Spot No. ^(a)	Protein	Plant species ^(b)	Accession number ^(c)	Exper. kDa/pI ^(d)	Theor. kDa/pI ^(e)	Mascot Score ^(f)	PM ^(g)	DB ^(h)	Ctrl ⁽ⁱ⁾	Fold change ^(j)			V%±SE ^(k)
										1 h	24 h	168 h	
Protein degradation													
1	Proteasome subunit beta type-6-like	<i>Glycine max</i>	gi 356507848	24.7/5.12	25.1/5.16	43	2	Ah	X	X	X	✓	
2	20S proteasome beta subunit	<i>Dimocarpus longan</i>	gi 339777225	25.8/6.09	29.0/6.54	61	6	Ah	✓	0.72	0.51	0.03	
(12)	Proteasome subunit beta type-6-like	<i>Glycine max</i>	gi 356507848	24.7/5.12	25.1/5.16	225	8	Ah	✓	0.50	0.25	0.44	
26	Proteasome subunit beta type-6-like	<i>Glycine max</i>	gi 356507848	24.6/5.31	25.1/5.16	231	11	Ah	✓	1.51	0.69	0.46	
62	Proteasome subunit beta type-1	<i>Vitis vinifera</i>	gi 225453909	24.1/6.46	24.6/6.88	172	8	Ah	✓	1.53	0.56	0.35	
(70)	Proteasome subunit alpha type-2-B	<i>Vitis vinifera</i>	gi 225423722	27.8/5.24	25.6/5.48	183	10	Ah	✓	0.59	0.34	0.23	
83	Proteasome beta type-3 subunit	<i>Spinacia oleracea</i>	gi 113624	24.1/5.12	38.4/5.96	216	3	Ah	X	✓	✓	✓	
92	Proteasome subunit beta type-1	<i>Vitis vinifera</i>	gi 225453909	24.3/6.48	24.6/6.88	375	9	Ah	✓	1.11	0.55	2.85	
94	Proteasome subunit beta type-1	<i>Vitis vinifera</i>	gi 225453909	24.5/6.64	24.6/6.88	209	5	Ah	✓	1.46	1.02	2.79	
Actin cytoskeleton organization													
56	Ama v 1.02 allergen (profilin)	<i>Amaranthus viridis</i>	gi 158389785	13.8/4.45	14.0/4.64	86	3	Ah	✓	2.09	3.34	2.71	
57	Ama v 1.01 allergen (profilin)	<i>Amaranthus viridis</i>	gi 158389783	14.3/4.40	14.2/4.46	34	3	Ah	✓	0.57	0.46	0.10	
86	Ama v 1.02 allergen (Profilin)	<i>Amaranthus viridis</i>	gi 158389785	13.2/4.58	14.0/4.64	74	3	Ah	✓	0.90	2.37	0.61	
(88)	Ama v 1.01 allergen (profilin)	<i>Amaranthus viridis</i>	gi 158389783	18.4/4.41	14.2/4.46	60	3	Ah	✓	2.21	1.61	0.30	
89	Ama v 1.01 allergen (Profilin)	<i>Amaranthus viridis</i>	gi 158389783	17.9/4.41	14.2/4.46	80	3	Ah	X	✓	✓	✓	
Cellular response to stress													
15	Nascent polypeptide-associated complex subunit α	<i>Vitis vinifera</i>	gi 225470846	29.3/4.37	22.0/4.34	436	7	Ah	✓	0.79	0.70	0.26	
24	Glutathione S-transferase-like protein	<i>Dianthus caryophyllus</i>	gi 390979559	25.3/6.32	23.0/6.19	104	4	Ah	X	X	✓	✓	
37	CBS domain protein	<i>Medicago truncatula</i>	gi 357491617	18.6/5.88	26.5/9.30	228	14	Ah	✓	1.41	3.23	0.80	
(41)	Alcohol dehydrogenase	<i>Dianthus caryophyllus</i>	gi 33149683	50.8/5.86	41.2/6.57	41	4	Ah	✓	0.55	1.78	0.29	
43	Gamma carbonic anhydrase	<i>Populus trichocarpa</i>	gi 224066191	29.1/6.08	29.4/6.18	88	5	Ah	✓	0.73	0.51	0.25	

Table 1. continued

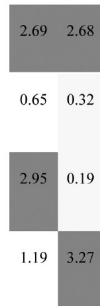
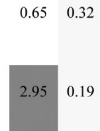
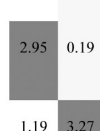
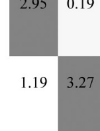
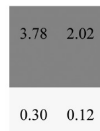
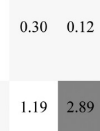
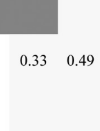
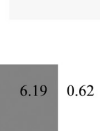
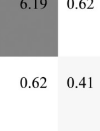
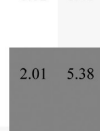
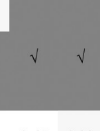
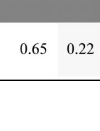
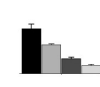
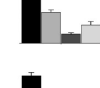
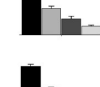
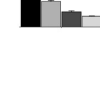
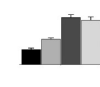
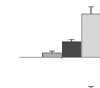
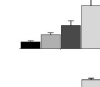
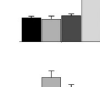
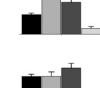
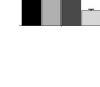
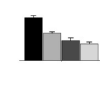
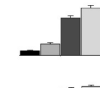
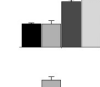
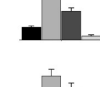
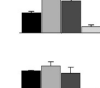
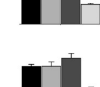
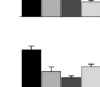
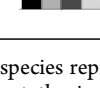
Spot No. ^(a)	Protein	Plant species ^(b)	Accession number ^(c)	Exper. kDa/pI ^(d)	Theor. kDa/pI ^(e)	Mascot Score ^(f)	PM ^(g)	DB ^(h)	Ctrl ⁽ⁱ⁾	Fold change ^(j)			V%±SE ^(k)
										1 h	24 h	168 h	
48	Copper/zinc superoxide dismutase	<i>Amaranthus hypochondriacus</i>	gi 296837079	17.0/5.43	15.3/5.27	158	3	NCBI	✓	1.45	2.69	2.68	
49	Ah24	<i>Amaranthus hypochondriacus</i>	gi 357942608	18.9/5.49	17.7/5.45	301	4	NCBI	✓	0.73	0.65	0.32	
71	Ah24	<i>Amaranthus hypochondriacus</i>	gi 357942608	20.7/4.94	17.7/5.45	74	2	NCBI	✓	1.11	2.95	0.19	
91	Glutathione S-transferase-like protein	<i>Dianthus caryophyllus</i>	gi 390979559	25.5/6.62	23.0/6.19	252	6	Ah	✓	1.24	1.19	3.27	
Amino acids, fatty acids and vitamin biosynthesis and metabolism													
10	Beta-hydroxyacyl-(Acyl-Carrier-Protein) dehydratase FabZ	<i>Helianthus annuus</i>	gi 302634224	20.8/4.77	25.1/8.82	86	3	Ah	✓	1.29	3.78	2.02	
23	Beta-hydroxyacyl-(Acyl-Carrier-Protein) dehydratase Fabz	<i>Helianthus annuus</i>	gi 302634224	20.9/5.07	25.1/8.82	46	4	Ah	✓	0.75	0.30	0.12	
(45)	Threonine syntase, chloroplastic-like isoform 1	<i>Solanum lycopersicum</i>	gi 460379654	59.0/6.00	57.3/6.54	198	10	Ah	✓	0.30	1.19	2.89	
(45)	Alanine aminotransferase 2	<i>Vitis vinifera</i>	gi 359482440	59.0/6.00	57.8/5.56	38	2	Ah	✓	0.30	1.19	2.89	
(53)	6,7-dimethyl-8-ribityllumazine synthase	<i>Beta vulgaris</i>	gi 282722285	14.9/6.54	23.7/8.26	104	9	Ah	✓	0.84	0.99	3.09	
54	6,7-dimethyl-8-ribityllumazine synthase	<i>Beta vulgaris</i>	gi 282722285	15.8/6.54	23.7/8.26	79	3	Ah	X	X	✓	✓	
55	6,7-dimethyl-8-ribityllumazine synthase	<i>Beta vulgaris</i>	gi 282722285	14.9/6.56	23.7/8.26	97	5	Ah	X	X	✓	✓	
(72)	3-isopropylmalate dehydratase small subunit-like	<i>Solanum lycopersicum</i>	gi 460392785	25.6/4.72	27.1/6.52	336	10	Ah	✓	3.74	2.29	0.31	
77	Glutamate dehydrogenase	<i>Ricinus communis</i>	gi 255568914	49.1/6.53	44.5/6.33	361	12	Ah	✓	0.69	0.33	0.49	
78	Eukaryotic translation initiation factor 3 subunit I-like	<i>Glycine max</i>	gi 356497716	38.8/6.56	35.8/6.84	218	12	Ah	✓	0.74	0.24	0.36	
Physiological defense response													
9	MLP-like protein 28	<i>Theobroma cacao</i>	gi 508709118	17.0 6.17	17.4/5.31	118	5	Ah	✓	2.29	6.19	0.62	
19	23 kDa Jasmonate-induced protein	<i>Zea mays</i>	gi 226494771	22.5/5.50	23.0/9.13	55	10	Ah	✓	0.96	0.62	0.41	
31	Jasmonate-induced protein homolog	<i>Atriplex canescens</i>	gi 1170595	19.2/6.08	19.5/5.26	53	3	Ah	✓	1.61	2.01	5.38	
32	Jasmonate-induced protein homolog	<i>Atriplex canescens</i>	gi 1170595	19.2/6.05	19.5/5.26	38	2	Ah	X	X	✓	✓	
51	Major latex like protein homolog	<i>Beta vulgaris</i>	gi 14594813	17.2/6.44	17.1/5.09	142	8	Ah	X	✓	✓	✓	
58	Jacalin-like plant lectin domain containing protein	<i>Aegilops tauschii</i>	gi 475627874	17.5/4.84	19.3/6.58	114	4	Ah	✓	0.64	0.65	0.22	

Table 1. continued

Spot No. ^(a)	Protein	Plant species ^(b)	Accession number ^(c)	Exper. kDa/pI ^(d)	Theor. kDa/pI ^(e)	Mascot Score ^(f)	PM ^(g)	DB ^(h)	Ctrl ⁽ⁱ⁾	Fold change ^(j)			V%±SE ^(k)
										1 h	24 h	168 h	
61	Jacalin-like plant lectin domain containing protein	<i>Aegilops tauschii</i>	gi 475627874	16.9/4.84	19.3/6.58	69	2	Ah	✓	0.64	0.33	0.18	
85	Pathogenesis-related protein	<i>Spinacia oleracea</i>	gi 444792485	19.4/5.10	17.9/4.72	117	11	Ah	✓	0.64	0.19	0.38	
90	Jacalin-like plant lectin domain containing protein	<i>Aegilops tauschii</i>	gi 475627874	16.9/4.87	19.3/6.58	93	3	Ah	✓	0.56	0.34	0.19	
97	Jacalin-like plant lectin domain containing protein	<i>Aegilops tauschii</i>	gi 475627874	16.5/4.72	19.3/6.58	138	3	Ah	✓	0.54	0.32	0.23	
Detoxification													
20	Cyanate hydratase	<i>Sorghum bicolor</i>	gi 242039407	17.1/5.90	18.6/5.29	163	5	Ah	✓	1.69	3.15	2.98	
21	Cyanate hydratase	<i>Sorghum bicolor</i>	gi 242039407	17.4/5.90	18.6/5.29	80	4	Ah	X	✓	✓	✓	
63	Lactoylglutathione lyase/glyoxalase I family protein	<i>Theobroma cacao</i>	gi 508701864	19.5/4.41	16.8/4.81	373	8	Ah	✓	2.02	3.34	6.19	
(80)	Lactoylglutathione lyase/glyoxalase I family protein	<i>Glycine max</i>	gi 356531939	40.9/5.70	33.4/6.13	153	11	Ah	✓	0.94	1.09	2.06	
(88)	Lactoylglutathione lyase/glyoxalase I family protein	<i>Theobroma cacao</i>	gi 508701864	18.4/4.41	16.8/4.81	148	5	Ah	✓	2.21	1.61	0.30	
(98)	Lactoylglutathione lyase/glyoxalase I family protein	<i>Theobroma cacao</i>	gi 508701864	18.3/4.46	16.8/4.81	261	5	Ah	✓	1.00	1.22	0.40	
Other processes													
(4)	Cupin 5 superfamily protein	<i>Populus trichocarpa</i>	gi 224069168	23.4/5.54	21.2/5.04	109	6	Ah	✓	0.64	0.46	0.39	
47	40S ribosomal protein S21-2-like isoform 1	<i>Solanum lycopersicum</i>	gi 460366746	11.9/6.60	11.2/7.78	80	2	Ah	✓	2.49	8.25	10.4	
64	Succinyl-CoA ligase [ADP-forming] subunit beta	<i>Sorghum bicolor</i>	gi 242062364	51.5/5.17	45.1/5.99	586	21	Ah	✓	0.99	1.95	2.10	
(72)	SOUL heme-binding protein	<i>Prunus persica</i>	gi 462407849	25.6/4.72	25.3/4.85	65	6	Ah	✓	3.74	2.29	0.31	
(88)	Probable Histone H2B.1-like	<i>Cucumis sativus</i>	gi 449450686	18.4/4.41	16.6/10.0	93	2	Ah	✓	2.21	1.61	0.30	
93	Regulator of ribonuclease-like protein 3-like isoform 1	<i>Cucumis sativus</i>	gi 449461084	17.9/5.76	17.7/5.90	103	3	Ah	✓	1.12	0.94	0.48	
(98)	Probable Histone H2B.1-like	<i>Cucumis sativus</i>	gi 449450686	18.3/4.46	16.6/10.0	39	2	Ah	✓	1.00	1.22	0.40	
99	Miraculin-like protein	<i>Vitis vinifera</i>	gi 359491783	18.3/5.7	23.8/6.15	133	6	Ah	✓	0.53	0.40	0.64	

^aSpot numbers as indicated in Figure 3; spot numbers in brackets indicate that the same spot matched to distinct proteins. ^bPlant species represent the most likely orthologous organisms. ^cAccession numbers according to NCBI nr database. When the best matches were against the in-house *Amaranthus hypochondriacus* transcriptome database, the most likely orthologous obtained after BLASTX against the NCBI nr database are reported. ^dExperimental mass (kDa) and pI of identified protein spots. ^eTheoretical mass (kDa) and pI of identified proteins retrieved from NCBIInr database or after calculation using the Compute pI/Mw tool (http://web.expasy.org/compute_pi/). ^fMascot score reported after database search. Individual ion scores >33 (for *Amaranthus hypochondriacus* transcriptome database), >43 (for the *Viridiplantae* subset of the NCBIInr database) are statistically

Table 1. continued

significant ($P < 0.01$). ^gNumber of peptides matched. ^hDatabase. Ah = *Amaranthus hypochondriacus* transcriptome database; NCBI = *Viridiplantae* subset of the NCBI nr database. ⁱPresence or absence of protein spots at control conditions (0 h) are indicated by ✓ and X respectively. ^jFold change is expressed as a ratio of the vol % between 150 mM NaCl-treated at different times/control roots, and each value represents the mean value of three biologically independent measurements. For some spots, fold change cannot be accurately calculated because of a complete absence of the spot in either treated or control samples; this is noted by the symbols ✓ and X, indicating the presence or absence of the spot, respectively. ^kProtein spot accumulation changes in *Amaranthus cruentus* roots proteins subjected to 150 mM NaCl at different times/control. Each column represents the mean value of three biologically independent measurements. Error bars indicate \pm standard error (SE).

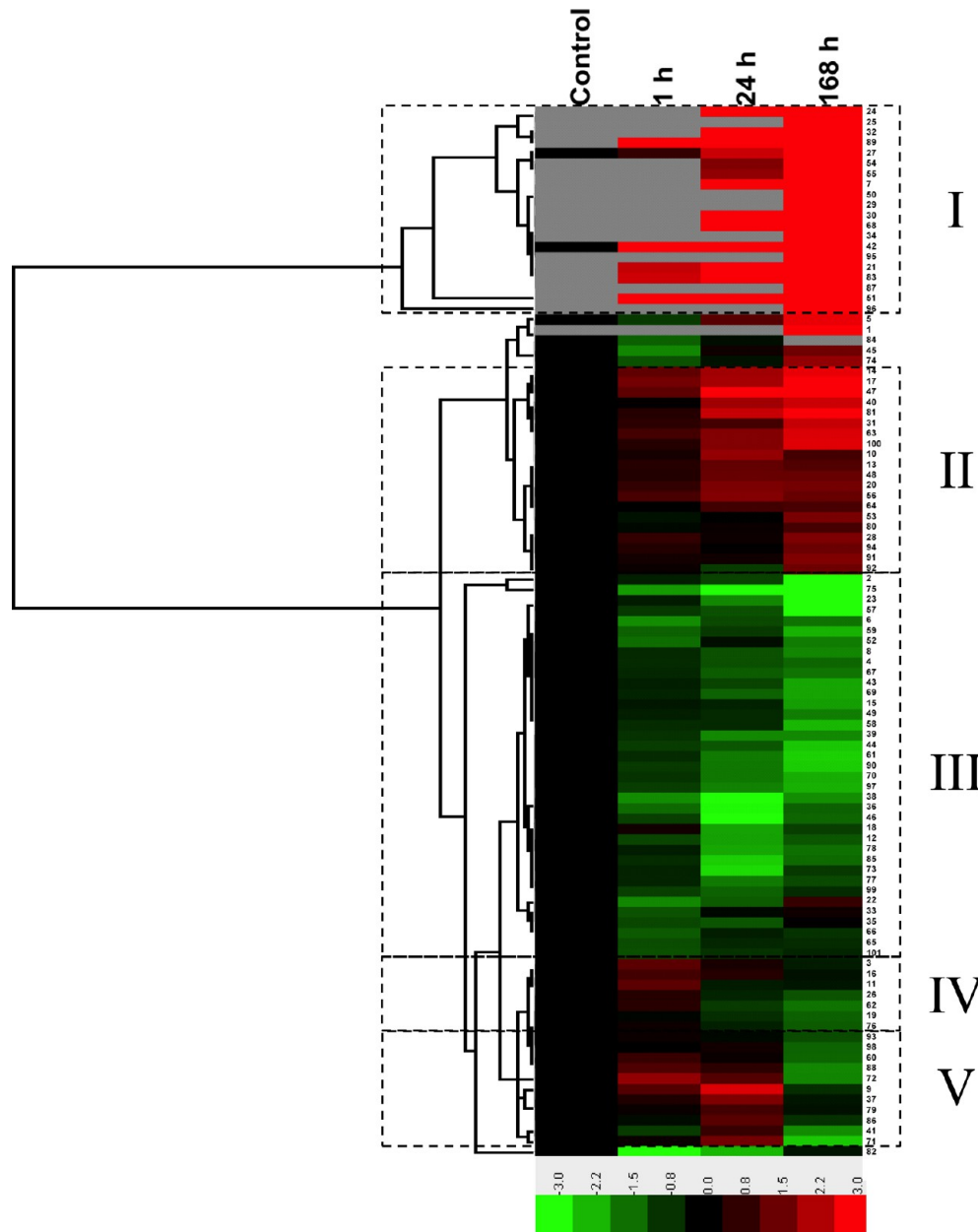


Figure 4. Hierarchical clustering of differentially accumulated amaranth root protein spots in response to salt stress. The four columns represent controls, and plants subjected to 150 mM NaCl for 1, 24 and 168 h, respectively. Rows represent individual protein spots. Protein spots not detected at any of the conditions are indicated in gray. Increased and decreased spot abundance ratios at the different time points of stress compared to controls are indicated in red or green, respectively. Spot numbers are shown on the right side. Dotted black boxes indicate protein spot clusters with similar abundance change patterns during the experiment.

spot 68) were highly homologous to chloroplastic-like proteins, suggesting the presence of these plastidial forms in amaranth roots. During evolution, most of the plastid genes were transferred to the nuclear genome, but not all their encoded

proteins appear to be imported into the plastid because they lack predictable N-terminal transit peptides.²⁸ Sequence analysis for the prediction of transit and signal peptides in these three amaranth proteins and their homology-based most

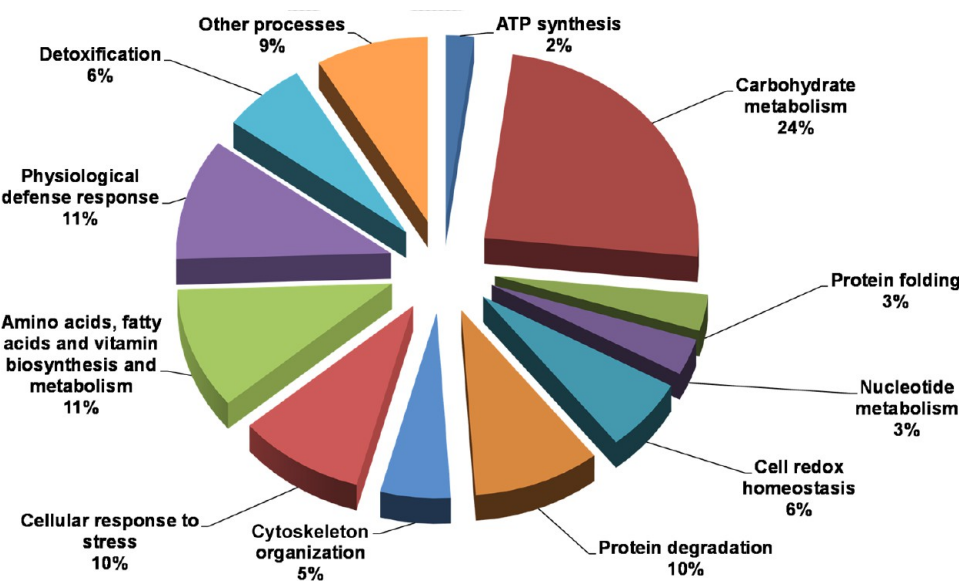


Figure 5. Classification of the identified proteins, the pie chart shows the distribution of the salt stress-responsive proteins into their biological process in percentage according to Gene Ontology (<http://www.geneontology.org/>).

likely orthologous proteins reported in this work (Table 1) was performed with the tool TargetP 1.1 server²⁹ (Supporting Information Figure S5). The tool predicted the presence of chloroplast transit peptides in two of the three most likely orthologous protein sequences, whereas in one case, a mitochondrial targeting peptide was identified. In all cases, a predicted cleavage site for the transit/targeting peptide was identified. The software predicted the presence of transit/targeting peptides in only one of the three amaranth protein sequences, and the same amino acid residue was predicted as the cleavage site. Even when TargetP is a successful prediction program for plastid proteins (70–85% of known plastid proteins), a significant number of plastid proteins will not be identified by this type of analysis.³⁰ On the basis of these results, we can only speculate about the differential accumulation of proplastidial root proteins in salt-stressed amaranth.

Identified proteins were grouped into different categories of biological processes (1. ATP synthesis, 2. Carbohydrate metabolism, 3. Protein folding, 4. Nucleotide metabolism, 5. Cell redox homeostasis, 6. Protein degradation, 7. Actin cytoskeleton organization, 8. Cellular response to stress, 9. Biosynthesis and metabolism of amino acids, fatty acids and vitamins, 10. Physiological defense response, 11. Detoxification, 12. Other processes), in which they are involved according to Gene Ontology (Figure 5). Many of the stress-responsive proteins were found to be redundant; the identification of such isoforms with a change in pI and/or molecular weight strongly suggests the salt stress-induced posttranslational modification and translation from alternatively spliced mRNAs of the candidate proteins, potentially including isoforms of multigenic families of proteins.

ATP Synthesis Proteins

Under salt-stress conditions, the osmotic and ionic phases of stress influence many of the processes and pathways at plant level and also within the cells. In cells of the root tissues, mitochondria are the main cellular compartment responsible for ATP production.³¹ In addition to its function in mitochondrial oxidative phosphorylation, a new role for ATP

synthase beta subunit as a pro-cell-death protein has been established as well as its function as a key negative regulator of plant cell death.³² Spots 25 and 66 were identified as ATP synthase beta subunit I (Figure 3, Table 1), interestingly showing contrasting accumulation patterns, whereas one spot significantly decreased under the osmotic phase of stress (after 1 h of stress imposition), the other appears only in the ionic phase of stress (after 168 h). Increased levels of ATP synthase subunit beta were observed in pea during abiotic stresses,³³ whereas the decrease of beta subunit of ATP synthase was reported under salt stress in tomato seedlings³⁴ and rice.³⁵

Carbohydrate Metabolism Proteins

Differential accumulation of proteins involved in different aspects of carbohydrate metabolism such as the glycolysis pathway was detected in *A. cruentus* roots under salt stress. In 13 individual spots (Figure 3, Table 1), differential accumulation was observed in four proteins related to glycolysis (fructokinase, fructose-bisphosphate aldolase, enolase, and triosephosphate isomerase). Enhanced glycolysis and increased expression of related enzymes under abiotic stresses have been reported.³⁶ However, in the present study, most of the nine spots identified as fructose-bisphosphate aldolase were decreased in abundance in response to progressive salt stress. In rice, fructose-bisphosphate aldolase is involved in root growth stimulated by gibberellin A through activation of the glycolytic pathway, whereas down-accumulation of this enzyme may be responsible for the alteration of sugars and starch metabolism as well as for the growth inhibition in cucumber roots under salt stress.³⁷ Fructose-bisphosphate aldolase plays an important role in carbohydrate metabolism and in the production of triose phosphate derivatives important in signal transduction.³⁸ It has been shown that enolase is responsive to salt, drought, cold, and anaerobic stress in different plants; however in rice roots under salt stress, it was found to be decreased in abundance and even disappeared after 72 h of stress treatment.³⁹ In our experiment, enolase decreased in abundance after 24 h (spots 35 and 39) and increased after 168 h (Spot 80). Fructokinase was identified in two spots. Spot 67 decreased significantly under stress, whereas spot 96 appeared

only after 168 h of stress imposition. Three isoforms of fructokinase-2 were increased in pollen samples only in a tolerant rice genotype under salt stress. This might result in increased starch content in pollen, which would support pollen growth and development under salt stress.⁴⁰ In a similar way, the appearing of a fructokinase only in the ionic phase (after 168 h) of salt stress may also result in an increased starch content to support growth in *A. cruentus* roots under salt stress.

Seven spots representing the pyruvate dehydrogenase E1 component subunit beta, lactate/malate dehydrogenase family protein, mitochondrial-like malate dehydrogenase, chloroplastic-like malate dehydrogenase, and the mitochondrial NAD-dependent malate dehydrogenase were differentially accumulated in response to salt stress. Spot 67 was identified as a mixture of pyruvate dehydrogenase E1 component subunit beta plus fructokinase showing a decreasing pattern of accumulation in response to progressive salt stress. Pyruvate dehydrogenase E1 component subunit beta is one of the catalytically active enzymes of the pyruvate dehydrogenase complex involved in the formation of energy through the tricarboxylic acid cycle (TCA), and this enzyme was decreased in abundance under NaCl stress in cucumber roots.³⁷ Mitochondrial-like malate dehydrogenase (spot 79) involved in the TCA was significantly increased in roots after 24 h of salt stress. Malate dehydrogenases have been reported to be responsive to salt stress in *Pisum sativum* roots⁴¹ and *Arabidopsis thaliana* cell suspension cultures⁴² as well as by long-term salinity stress in *Thellungiella halophila* leaves⁴³ and in needle leaves of *Pinus halepensis* naturally subjected to NaCl stress.⁴⁴ Mitochondrial NAD-dependent malate dehydrogenase and chloroplastic-like malate dehydrogenase have been reported to be slightly accumulated after 6 h in response to salt stress in *A. thaliana* cell suspensions.⁴² In the present work, chloroplastic-like malate dehydrogenase (spot 65) was significantly decreased after 1 h of treatment, whereas two spots identified as mitochondrial NAD-dependent malate dehydrogenase showed a contrasting accumulation pattern; spot 44 decreased during all stages of stress imposition, and spot 95 only appeared after 168 h of stress.

Proteins Related to Protein Folding

Plants employ two strategies to cope with the misfolded proteins: one is the removal of such proteins and the other is to refold them. Three spots were identified as proteins implicated in protein folding (Table 1). Cyclophilins are a family of highly conserved proteins included into the immunophilins superfamily, in which many but not all the members possess peptidyl prolyl *cis-trans* isomerase (PPIase) or rotamase activity.⁴⁵ In wheat seedlings, the combined effect of heat shock and drought stress induced the accumulation as demonstrated by Western blot analysis of a 45 kDa cyclophilin. Some studies have established a correlation between cyclophilin overexpression and stress protection in plants and other organisms, for example, overexpression of a single domain, and nuclear localized cyclophilin isolated from *T. halophila* in BY2 tobacco cells and yeast provides multiple abiotic stress tolerance.⁴⁶ The overexpression of a rice cyclophilin gene, *OsCyp2*, has shown to enhance multiple stress tolerance in *E. coli* and *S. cerevisiae*.⁴⁷ Overexpression of a cotton cyclophilin in transgenic tobacco plants conferred tolerance to salt stress as well as enhanced tolerance to *Pseudomonas syringae* infection.⁴⁸ In *A. cruentus* roots, we found two salt stress-responsive cyclophilins (spots 3 and 22) that showed an interestingly opposite accumulation

pattern (Figure S2), strongly suggesting a posttranslational modification of this protein in response to salt stress. *A. cruentus* cyclophilins are potential candidates to be exploited for engineering stress tolerance in plants. Calreticulin is a Ca²⁺-binding protein resident mainly in the endoplasmic reticulum (ER), where it plays a major role in intracellular Ca²⁺ homeostasis and signaling and also serves as a chaperone to newly synthesized glycoproteins. Calreticulins have a function in growth and development as well as biotic and abiotic stress responses in plants.⁴⁹ Previous proteomic reports indicated that calreticulin accumulation decreased after 6 h by salt stress in *A. thaliana* roots,⁵⁰ calreticulin was also decreased in response to early salt stress in wild type and OSRK1 transgenic rice roots.⁵¹ On the contrary, in the present work, spot 60 was identified as a calreticulin showing a decreased accumulation after 168 h of stress imposition.

Nucleotide Metabolism Proteins

Spot 7, identified as a deoxyuridine 5'-triphosphate nucleotide-hydrolase (dUTP pyrophosphatase) appeared as a small spot after 24 h and increased its accumulation after 168 h of stress imposition (Figure S1). This enzyme hydrolyzes deoxyuridine-triphosphate (dUTP) to pyrophosphate and deoxyuridine-monophosphate (dUMP), the immediate precursor of thymidine nucleotides. Two nucleoside diphosphate kinases (NDPKs) were identified: spot 53 (NDPK1) increased only after 168 h of stress imposition, whereas spot 68 (NDPK4) appeared only after 24 h and increased its accumulation after 168 h of stress imposition. NDPKs play significant roles in hormone responses, hydrogen peroxide signaling, development and growth; they are recognized as stress-responsive proteins and are strongly expressed under abiotic stress conditions such as drought and salt stress. These roles are attributed to these proteins because of their phosphotransferase activity.^{47,52}

Cell Redox Homeostasis Proteins

Salt stress can accelerate the production of ROS, resulting in oxidative damage to DNA, lipids, and proteins. The harmful influence of ROS on cell macromolecules may also be alleviated by the activity of antioxidant compounds such as ascorbic acid, glutathione, thioredoxin, and carotenoids.⁵³ We found six proteins whose functions are implicated in cell redox homeostasis (Table 1). These include three enzymes also related to the protection of cells to oxidative damage such as dehydroascorbate reductase (spots 4 and 14), monodehydroascorbate reductase (spot 45), and thioredoxin-h (Trx-h, spot 52). Ascorbate is a very important antioxidant molecule in plants, this molecule is consumed by ascorbate peroxidase to detoxify H₂O₂, while generating two molecules of monodehydroascorbate (MDHA) that is converted to dehydroascorbate (DHA). Conversion of MDHA and DHA to ascorbate is catalyzed by monodehydroascorbate reductase and dehydroascorbate reductase, respectively. Instant reduction of MDHA and DHA is crucial to maintenance of a proper ascorbate pool.⁵⁴ In the present work, spot 52 identified as a Trx-h decreased in abundance after 1 h, recovered almost to abundance similar to controls, and decreased again after 168 h of stress imposition. Only few predicted functions of Trx-h have been elucidated; it has been reported that low molecular weight forms of Trx-h function as disulfide reductase, although high molecular weight forms function as chaperone.⁵⁵ Trx-h overexpression in *Nicotiana tabacum* conferred resistance to tobacco and cucumber mosaic virus and also enhanced tobacco resistance to abiotic oxidative stress.⁵⁶ Enigmatically, overexpression of a

rice low molecular weight Trx-h, previously reported as increased under salt stress in rice apoplast,⁵⁷ resulted in a salt-sensitive phenotype.⁵⁸

Proteins Related to Protein Degradation

The selective breakdown of most of the regulatory proteins by the ATP-dependent ubiquitin-proteasome pathway controls important aspects of plant development, growth, and response to biotic and abiotic stress. In *A. cruentus* roots, five proteins involved in protein degradation were found, only one (spot 1) of the three spots identified as the proteasome subunit beta type-6-like appeared after 168 h of stress, whereas the other two spots (spots 12 and 26) as well as the proteasome subunit alpha type-2-B (spot 70) decreased under salt stress. Interestingly, proteasome beta type-3 subunit (spot 83), which was absent in control, was significantly accumulated after stress imposition, reaching its highest accumulation after 168 h. Increased accumulation of proteasome beta type 1 subunits and decreased accumulation of 20S proteasome subunits are among the major changes revealing differential protein abundance under salinity between glycophytes and halophytes.⁵⁹ In this work, two of the three spots identified as the proteasome subunit beta type-1 (spots 92 and 94) showed significant accumulation, whereas one (spot 62) was significantly decreased after 168 h of stress imposition. The 20S proteasome beta subunit (spot 2) was significantly decreased after 168 h of stress imposition. The 20S proteasome is responsible for the ATP-independent degradation of oxidized proteins. Under oxidative stress, the proteasomal system must adapt to ensure a regulatory response and degradation of oxidized proteins.⁶⁰ Plant cells contain a mixture of 26S and 20S proteasomes, 26S proteasome levels are needed to maintain tolerance to stress, although elevated levels of free 20S proteasome increase tolerance to oxidative stress. Regulation of the 26S and 20S proteasome ratio is important for plant development and stress responses.⁶¹ The ROS concentrations required to produce oxidative damage seem to be different for halophytes and glycophytes. For some halophytes increased in lipid peroxidation, an indication of oxidative stress occurred only when salt concentration exceeded 150 mM.⁶² Increased relative abundance of some proteasome subunits has been found in halophytes taxonomically related to *A. cruentus*, for example, proteasome subunit alpha type 6 in *S. aegyptiaca*⁶³ or 26S proteasomal subunit in *S. europaea*,⁶⁴ indicating an enhanced protein degradation upon salt stress.

Proteins Related to Actin Cytoskeleton Organization

Profilins are ubiquitous low-molecular-weight (12–15 kDa) proteins, which bind actin monomer and cause polymerization or depolymerization of actin filaments. Cytoskeleton remodeling resulted from polymerization, and depolymerization of actin filaments induces plant cells to spatially and temporally respond to internal and external signals.⁶⁵ The cytoskeleton is involved in the SOS (salt overly sensitive) signaling pathway, Ca²⁺ influx, and some regulatory mechanisms of salt-induced cytoskeleton-associated proteins.⁶⁶ Two profilins (Ama v 1.01 and Ama v 1.02) were identified in five different protein spots (56, 57, 86, 88, and 89). Four of these five spots were increased in response to salt stress in accordance with previous reports in plants belonging to the family Amaranthaceae such as *S. aegyptiaca*⁶³ and *S. europaea*.⁶⁴ Notably, spot 89, which was absent under control conditions, was only detectable after stress imposition. However, spot 57 was significantly decreased at all times in response to salt stress in *A. cruentus* roots.

Proteins Related to Cellular Response

Nine of the differentially accumulated protein spots were classified as directly involved in the cellular response to salt stress (Table 1). Among them, cooper-zinc superoxide dismutase (SOD^{Cu-Zn}, spot 48) and glutathione S-transferase (spots 24 and 91), widely known as antioxidant enzymes, were significantly accumulated in response to salt stress in *A. cruentus* roots. The increased accumulation of glutathione S-transferase in response to salt and osmotic stress has been extensively reported before.⁴² The increased accumulation of SOD^{Cu-Zn} in amaranth roots in response to abiotic stress conditions has been observed previously.¹⁹ Several reports also mentioned the increased accumulation of SOD^{Cu-Zn} under-salt stress conditions.^{42,66–69}

In this work, alcohol dehydrogenase (spot 41) decreased in response to 168 h of salt stress imposition. Alcohol dehydrogenase protein accumulation increased in soybean hypocotyls in response to salt stress, indicating that the main role of this enzyme is to produce ATP and consume glycolytic products under salt stress.⁷⁰ However, the abundance of alcohol dehydrogenase transcript in the roots of the halophyte grass model *Spartina alterniflora* was down-regulated up to 90 min in response to salt stress, and then the amount was higher than the unstressed controls. The role of alcohol dehydrogenase in response to salt stress is not clearly understood; however, the crosstalk between the alcohol fermentation pathway and one of the salt-tolerance mechanisms needs to be investigated.⁷¹

Nascent polypeptide-associated complex alpha subunit (NAC α , spot 15) was significantly decreased in abundance after 168 h of stress imposition. The decreased accumulation of NAC α might affect gene transcription, protein translation, and targeting leading to metabolic disorders.³⁹ NAC α was also decreased in leaves of two genotypes of sugar beet under drought stress⁷² and in rice roots subjected to salt stress in the presence of 150 mM NaCl, where NAC α may represent a novel target to salt toxicity.³⁹ Amaranth's NAC α may be an interesting candidate gene/protein to overexpress in order to confer abiotic stress tolerance in other crops. Carbonic anhydrases are zinc-containing enzymes that catalyze the interconversion of carbon dioxide and water into bicarbonate and protons. Carbonic anhydrases are abundant in plants and unicellular green algae, where they are essential for photosynthetic CO₂ fixation.⁷³ Carbonic anhydrases are divided into five distinct families (alpha, beta, gamma, delta, and epsilon), which have no primary sequence homology and appear to have evolved independently.⁷³ Gamma carbonic anhydrases are widely spread among archaea, bacteria, and eukaryotic photosynthetic organisms and are involved in complex I assembly in mitochondria and respiration. Spot 43, identified as a gamma carbonic anhydrase, was significantly decreased in response to salt stress. Interestingly, transgenic *A. thaliana* exhibited salt tolerance when it overexpressed the *OsCA1* gene coding for a rice carbonic anhydrase induced by salt and osmotic stress.⁷⁴

It has been demonstrated that proteins consisting of a single cystathionine β -synthase (CBS) domain pair stabilize cellular redox homeostasis and modulate plant development via regulation of thioredoxin systems by sensing changes in adenosine-containing ligands such as AMP, ATP, or NADPH and help to regulate the enzymatic activity of adjacent domains.⁷⁵ Spot 37, a CBS domain-containing protein was significantly increased after 24 h of salt stress imposition in amaranth roots. Interestingly transgenic tobacco plants over-

expressing a rice gene (*OsCBSX4*) encoding for a CBS domain protein, exhibited improved tolerance to salt, heavy metal, and oxidative stress. Such transgenic plants accumulated less Na⁺ and were also able to grow and produce seeds under the presence of 150 mM NaCl.⁷⁶

Ah24 is one of the several genes with unknown function obtained during the first large transcriptomic analysis of amaranth plants subjected to biotic and abiotic stress conditions. The protein coded by this gene seems to be a new modulator of the jasmonic acid-mediated response to mechanical damage and herbivory.⁷⁷ This gene/protein, which is unique in amaranth, is currently being functionally characterized in tobacco and *A. thaliana*.^{77,78} In this work, two spots were identified as the *Ah24* protein: spot 49 was significantly decreased after 168 h of stress imposition, whereas spot 71 was significantly increased after 24 h and decreased after 168 h of stress imposition. These results suggest that *Ah24* is also responsive to salt stress and should be regulated at the posttranslational level.

Proteins Related to the Biosynthesis and Metabolism of Amino Acids, Fatty Acids, and Vitamins

The abundance of glutamate dehydrogenase (spot 77) and the eukaryotic translation initiation factor 3 subunit I-like (spot 78) decreased after 24 and 168 h, whereas the abundance of the spot 45, identified as a mixture of alanine aminotransferase 2 and threonine synthase, decreased after 1 h and increased significantly after 168 h. Spots 10 and 23 were identified as the beta-hydroxyacyl-acyl carrier protein dehydratase (FabZ) showed opposite accumulation patterns after 24 and 168 h, suggesting the salt stress-induced posttranslational modification of this protein in amaranth roots. The FabZ efficiently catalyzes the dehydration of short chain beta-hydroxyacyl-acyl carrier proteins and long chain saturated and unsaturated beta-hydroxyacyl-acyl carrier proteins.⁷⁹ FabZ protein and transcript have been decreased under aluminum stress in tomato roots⁸⁰ and under salt stress in *Medicago truncatula* roots,⁸¹ respectively.

Spot 72 (3-isopropylmalate dehydratase small subunit-like) was significantly increased after 1 and 24 h and decreased after 168 h of stress imposition. Three spots identified as the lumazine synthase (6,7-dimethyl-8-ribityllumazine synthase) were significantly increased in response to salt stress (spots 53, 54, and 55, Table 1, Figure S2). It is noteworthy that two of them were absent in controls and appeared after 24 h of stress imposition. Riboflavin (vitamin B₂) is the precursor of flavin mononucleotide and flavin adenine dinucleotide, which are two key cofactors involved in a wide variety of redox processes. Lumazine synthase catalyzes the penultimate step in the biosynthesis of riboflavin in plants and microorganisms.⁸² The expression of the *COS1* gene encoding a lumazine synthase helped to demonstrate that a novel function for the riboflavin pathway acting downstream of jasmonate-signaling coronatine insensitive 1 (COI1) in the jasmonate signaling pathway and is required for suppression of the COI1-mediated root growth, senescence, and plant defense.⁸³ Interestingly, spots 54 and 55 (lumazine synthase) appeared after 24 h suggest that the signals for root growth inhibition were triggered before the first 24 h of salt stress imposition.

Proteins Related to Physiological Defense Response

Changes in the abundances of proteins related to defense responses were also found in this work. Three spots were identified as proteins containing the ligand-binding Bet v1

domain of major pollen allergen of white birch (*Betula verrucosa*). Spot 85 was identified as a pathogenesis-related protein and decreased in response to salt stress. Pathogenesis-related proteins have been well-defined as plant proteins that are induced not only during pathogen infection but also in response to abiotic stresses, including wounding, drought, and high salinity.⁸⁴ Pathogenesis-related proteins accumulation increased significantly under salt stress in salt-tolerant peanut,⁸⁵ salt-tolerant barley roots⁸⁶ and in seedling roots of salt-tolerant wheat.⁶ Spots 9 and 51 were identified as major latex proteins, the former significantly increased after 1 and 24 h, whereas the last was absent in controls but appeared after 1 h and reached its maximum accumulation after 24 h of stress imposition. The role of major latex proteins is unclear; however, they are associated with fruit and flower development and in pathogen defense responses. A number of pathogenesis-related proteins including the Bet v1 domain, have RNase activity in vitro. The biological significance of such activity is unclear, and several of them are also allergenic.⁸⁷ The expression of a gene that encodes a protein similar to members of the major latex proteins subfamily in the Bet v1 family was induced by salt stress in cotton roots. Salt tolerance was significantly enhanced in transgenic *A. thaliana* expressing this major latex protein.⁸⁸

We have also identified four spots as Jacalin-like plant lectin domain containing proteins all significantly decreased in response to salt stress. Jacalin-related lectins are a subgroup of proteins that have one or more domains with sequences similar to the jacalin protein isolated from jackfruit (*Artocarpus integrifolia*). The majority of jacalins are mannose-specific lectins and the rest are galactose-specific lectins.⁸⁹ The significant accumulation of a mannose-binding lectin was reported in rice roots after 10 and 24 h of stress imposition,⁹⁰ although in soybean hypocotyl and root, a lectin-like protein decreased in abundance after 72 h of salt stress imposition with 100 mM NaCl.⁹¹ Despite the apparent association of jacalins with plant defense, their functions remain elusive, particularly due to their structural diversity.⁹² Jasmonates are plant modulators of the expression of numerous genes and mediate responses to stress, wounding, insect attack, pathogen infection, and UV damage. They also play key roles in reproduction and regulate many plant developmental processes.⁸³ Three jasmonate-induced proteins were identified in this work; the spot 19 (23 kDa jasmonate-induced protein) decreased in abundance after 24 and 168 h of stress imposition. Under salinity stress, a 23 kDa jasmonate-induced protein decreased in abundance in the roots of two contrasting barley genotypes.⁹³ Spots 31 and 32 identified as a 19 kDa jasmonate-induced protein homolog; the first increased after 24 and 168 h, whereas the second was absent in controls and appeared after 24 of stress imposition (Table 1).

Detoxification Related Proteins

Function and biochemical characteristics of plant cyanases (also known as cyanate lyases, cyanate hydrolases, or cyanate hydratases) are poorly studied. However, the role of the plant cyanases is likely to detoxify the cyanate, but it is also possible that the cyanase-catalyzed catabolism of cyanate provides the plant with nitrogen and carbon dioxide. The up-regulation of the *S. aegyptiaca* cyanase indicates that cyanate is formed during salt accumulation.⁶³ It has been proved recently in *A. thaliana* that T-DNA insertion mutant lines for cyanase 7, ectopically expressing *A. thaliana* and rice cyanases exhibited resistance to KCNO stress, which demonstrated that one role of cyanases in

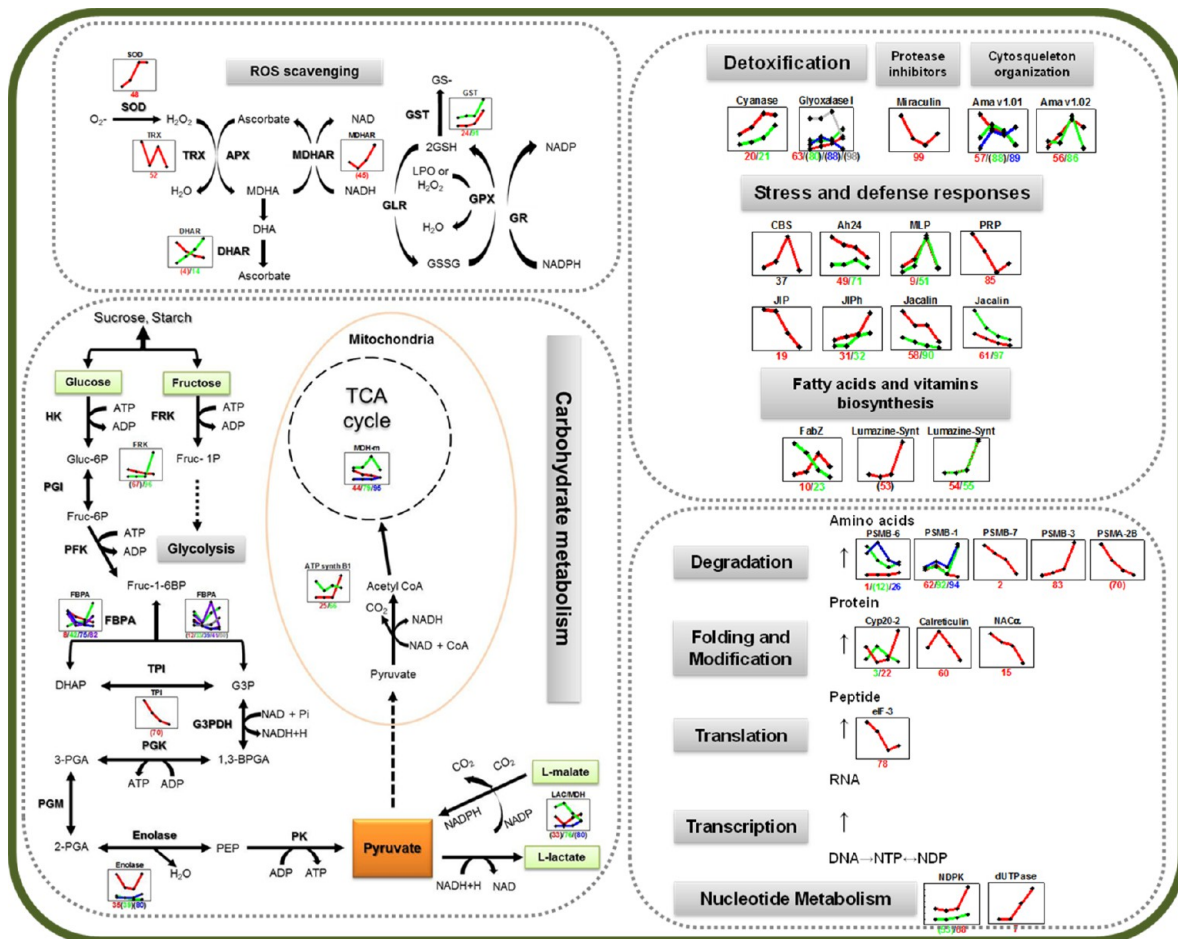


Figure 6. Schematic representation of salt stress-responsive mechanisms in *Amaranthus cruentus* roots. Protein accumulation patterns of the identified proteins are shown in graphs. When more than one line is shown in a mini-graph, the color of the line represents the spot number with the same color. Each point in the curve represents the control, and plants subjected to 150 mM NaCl for 1, 24, and 168 h, respectively. Abbreviations for metabolites: 1,3-BPGA, 1,3 bis phosphoglyceric acid; 2-PGA, 2 bis phosphoglyceric acid; 3-PGA, 3 phosphoglyceric acid; ADP, Adenosine diphosphate; ATP, Adenosine triphosphate; CoA, Coenzyme A; DHA, Dehydroascorbate; DHAP, Dihydroxyacetone phosphate; Fruc-1-6BP, Fructose 1,6 bisphosphate; Fruc-1P, Fructose 1 phosphate; Fruc-6P, Fructose 6 phosphate; G3P, Glyceraldehyde 3 phosphate; Gluc-6P, Glucose 6 phosphate; GSH, Reduced glutathione; GSSG, Oxidized glutathione; LPO, Lipoperoxide; MDHA, Monodehydroascorbate; NAD/NADH, Nicotinamide adenine dinucleotide; NADP/NADPH, Nicotiamide adenine dinucleotide phosphate; NDP, Nucleoside diphosphate; NTP, Nucleoside triphosphate; PEP, Phosphoenol pyruvate. Abbreviations for enzymes and other proteins: Ama v1.01, Amaranth profilin; Ama v1.02, Amaranth profilin; APX, Ascorbate peroxidase; ATPsynthB1, ATP synthase beta subunit 1; CBS, Cystathionine β -synthase domain protein; CYP20-2, Cyclophilin 20-2; DHAR, Dehydroascorbate reductase; dUTPase, deoxyuridine 5'-triphosphate nucleotidehydrolase; eIF-3, Eukarotic translation initiation factor 3; FabZ, Beta-hydroxyacyl-(ACP)dehydratase; FBPA, Fructose-bisphosphate aldolase; FRK, Fructokinase; G3PDH, Glyceraldehyde 3-phosphate dehydrogenase; GLR, Glutaredoxin; GPX, Glutathione peroxidase; GR, Glutathione reductase; GST, Glutathione S-transferase; HK, Hexokinase; JIP, Jasmonate-induced protein; JIPh, Jasmonate-induced protein homolog; LAC/MDH, Lactate/malate dehydrogenase family protein; Lumazine-Synt, 6,7-dimethyl-8-ribityllumazine synthase; MDHAR, Monodehydroascorbate reductase; MDH-m, Malate dehydrogenase mitochondrial-like; Miraculin, Miraculin-like protein; MLP, Major latex protein; NAc α , Nascent associated complex alpha subunit; NDPK, Nucleoside diphosphate kinase; PFK, Phosphofructokinase; PGI, Phosphoglucose isomerase; PGK, Phosphoglycerate kinase; PGM, Phosphoglycerate mutase; PK, Pyruvate kinase; PRP, Pathogenesis-related protein; PSMB, Proteasome subunit alpha type-2B; PSMB-1, Proteasome subunit beta type-1; PSMB-3, Proteasome subunit beta type-3; PSMB-6, Proteasome subunit beta type-6; PSMB-7, Proteasome subunit beta type-7; SOD, superoxide dismutase; TPI, Triosephosphate isomerase; TRX, Thioredoxin; Tryp-Inh, Trypsin inhibitor.

plants is detoxification. Transcription of the *A. thaliana* cyanase was not significantly affected by KCNO treatment but was induced by salt stress.⁹⁴ In this work, spots 20 and 21 were identified as cyanases, the first was significantly accumulated in response to salt stress, whereas the last was absent in controls and accumulated only in response to stress (Table 1, Figure S4). Increased accumulation of cyanases indicates that cyanate is formed during salt stress in amaranth roots. The stress-inducible cyanase (spot 21) with a slightly higher molecular weight identified in this work may be a posttranslational modification or a protein isoform induced by salt stress.

Methylglyoxal is generated from the oxidation of carbohydrates and lipids, and it can form adducts with proteins and nucleic acids, which is deleterious to cellular functions.⁹⁵ Plant concentrations of methylglyoxal are significantly increased under stress.⁹⁶ Glyoxalase I catalyzes the isomerization of the hemithioacetal formed spontaneously between methylglyoxal and reduced glutathione to (S)-D-lactoylglutathione, which can be converted to D-lactic acid and reduced glutathione by glyoxalase II. Regarding the enzymatic function, glyoxalase I is officially classified as a lactoylglutathione lyase. With respect to the subcellular localization, it is regarded to be a cytosolic

protein; a plausible scenario considering the major source of methylglyoxal (glycolysis). The sugar beet M14 glyoxalase I gene was up-regulated in response to salt, mannitol, and oxidative stresses. Heterologous expression of this protein could increase *E. coli* tolerance to methylglyoxal, whereas in transgenic tobacco plants constitutively expressing this glyoxalase I, both seedlings and leaf discs were significantly tolerant to methylglyoxal, salt, mannitol, and H_2O_2 . This demonstrates the importance of glyoxalase in abiotic stress tolerance and cellular detoxification.⁹⁷ In this work, spot 63 increased under salt stress, and spots 80, 88, and 98 were identified as lactoylglutathione lyase/glyoxalase I family proteins.

CONCLUSION

The hydroponic system used in this study has enabled us to magnify and clearly observe the osmotic effect on plants, as well as the recovery and the beginning of the ionic phase of stress, including a rapid collection of the materials to be analyzed. A schematic representation of the main salt stress-responsive mechanisms in *A. cruentus* roots derived from the changes observed in the proteome is shown in Figure 6. Changes in protein abundance revealed that to protect against oxidative damage and the generation of toxic components as result of stress conditions, increased accumulation of detoxifying enzymes and ROS scavenging enzymes are essential for amaranth survival. Alteration in carbohydrate-related and energy metabolism-related enzymes mainly decreased in amaranth under salt stress and are an indication that a satisfactory energy supplement is a requisite to cope with stress conditions. Different protein-folding proteins are accumulated in amaranth roots in response to the increased protein degradation occurring during stress. Proteins related to cytoskeleton organization are altered to maintain cell turgor under the different phases of salt stress. Proteins related to stress and defense responses whose overexpression has been shown to potentially confer tolerance to salinity and other abiotic stresses are also responsive in amaranth roots.

Our results also show a differential accumulation of proplastidial proteins in roots of salt-stressed amaranth. Although in recent years, several localization predictors for plant plastid proteins have been published, experiments targeting the specific identification of plastid proteins are necessary for an unquestionable identification of this type of proteins. Notably, many of the proteins identified in this work have been reported to be induced by salt and other abiotic stresses, and in some cases, the absence of such proteins have caused plants to become hypersensitive to stress damage; on the contrary, when overexpressed, such proteins have proven to confer tolerance to salinity and other abiotic stresses. However, functional complementation by heterologous expression in yeast or in insertional lines, among other strategies, is still necessary to demonstrate the role played by such stress-induced proteins in amaranth's responsive mechanisms to cope with abiotic stress. The role of isoforms or posttranslationally modified cyanases induced only in response to salt stress in amaranth roots deserves more attention. Amaranth is a stress tolerant and highly nutritious nonconventional crop that can fulfill the requirements of sustainable agriculture and food safety, and understanding its biochemical network associated with the stress defense will also stimulate the breeding of other crops for higher tolerance against abiotic stresses.

ASSOCIATED CONTENT

Supporting Information

This material is available free of charge via the Internet at <http://pubs.acs.org>.

AUTHOR INFORMATION

Corresponding Author

*E-mail: apbarba@ipicyt.edu.mx. Fax:+52-444-8342010. Tel.: 52-444-8342000.

Notes

The authors declare no competing financial interest.

ACKNOWLEDGMENTS

We thank CONACYT-MEXICO GRANT 56787 (Laboratory for Nanoscience and Nanotechnology Research-LINAN) and Waters-México. We thank Dr. John Paul Délano Frier (CINVESTAV-Irapuato) for the *Amaranthus hypochondriacus* transcriptome information. We also thank to Dr. Hugo Sergio Aguilar Hernández (DBM-IPICYT), Ms. C. Dulce Isela de Fátima Partida Gutiérrez (DCA-IPICYT), Verónica Zárate Chávez (LANBAMA-IPICYT) and Antonio Castellanos Martínez (CNS-IPICYT) for their valuable technical assistance.

ABBREVIATIONS:

CBS, cystathionine β -synthase; dUMP, deoxyuridine-monophosphate; dUTP, deoxyuridine-triphosphate; DW, dry weight; EC, electrical conductivity; ER, endoplasmic reticulum; EST, expressed sequence tag; FabZ, beta-hydroxyacyl-acyl carrier protein-dehydratase; NAC α , nascent associated complex alpha subunit; NDPK, nucleoside diphosphate kinase; PPIase, peptidyl prolyl *cis-trans* isomerase; ROS, reactive oxygen species; SOD $^{Cu-Zn}$, copper-zinc superoxide dismutase; SOS, salt overly sensitive; TCA, tricarboxylic acid cycle; Trx-h, thioredoxin-h

REFERENCES

- (1) Tester, M.; Davenport, R. Na⁺ Tolerance and Na⁺ Transport in Higher Plants. *Ann. Bot.* **2003**, *91* (5), 503–527.
- (2) Wang, W.; Vinocur, B.; Altman, A. Plant responses to drought, salinity and extreme temperatures: towards genetic engineering for stress tolerance. *Planta* **2003**, *218* (1), 1–14.
- (3) Munns, R.; Tester, M. Mechanisms of salinity tolerance. *Annu. Rev. Plant Biol.* **2008**, *59*, 651–81.
- (4) Valliyodan, B.; Nguyen, H. T. Understanding regulatory networks and engineering for enhanced drought tolerance in plants. *Curr. Opin. Plant Biol.* **2006**, *9* (2), 189–195.
- (5) Witzel, K.; Weidner, A.; Surabhi, G.-K.; Börner, A.; Mock, H.-P. Salt stress-induced alterations in the root proteome of barley genotypes with contrasting response towards salinity. *J. Exp. Bot.* **2009**, *60* (12), 3545–3557.
- (6) Guo, G.; Ge, P.; Ma, C.; Li, X.; Lv, D.; Wang, S.; Ma, W.; Yan, Y. Comparative proteomic analysis of salt response proteins in seedling roots of two wheat varieties. *J. Proteomics* **2012**, *75* (6), 1867–1885.
- (7) Zhao, Q.; Zhang, H.; Wang, T.; Chen, S.; Dai, S. Proteomics-based investigation of salt-responsive mechanisms in plant roots. *J. Proteomics* **2013**, *82*, 230–253.
- (8) Ghosh, D.; Xu, J. Abiotic stress responses in plant roots: a proteomics perspective. *Front. Plant Sci.* **2014**, *5*, 6.
- (9) Espitia-Rangel, E.; Mapes-Sánchez, C.; Escobedo-López, D.; De la O-Olán, M.; Rivas-Valencia, P.; Martínez-Trejo, G.; Cortés-Espinoza, L.; Hernández-Casillas, J. *Conservación y uso de los recursos genéticos del amaranto en México*; SINAREFI-INIFAP-UNAM: Celaya, Guanajuato, México, 2010; Vol. 1, p 201.

- (10) Omami, E. N.; Hammes, P. S. Interactive effects of salinity and water stress on growth, leaf water relations, and gas exchange in amaranth (*Amaranthus* spp.). *N. Z. J. Crop Hortic. Sci.* **2006**, *34* (1), 33–44.
- (11) Barba de la Rosa, A. P.; Fomsgaard, I. S.; Laursen, B.; Mortensen, A. G.; Olvera-Martínez, L.; Silva-Sánchez, C.; Mendoza-Herrera, A.; González-Castañeda, J.; De León-Rodríguez, A. Amaranth (*Amaranthus hypochondriacus*) as an alternative crop for sustainable food production: Phenolic acids and flavonoids with potential impact on its nutraceutical quality. *J. Cereal Sci.* **2009**, *49* (1), 117–121.
- (12) Barba de la Rosa, A. P.; Silva-Sánchez, C.; González de Mejia, E. Amaranth: An Ancient Crop for Modern Technology. In *Hispanic Foods*; Tunick, M. H., Gonzalez de Mejía, E., Eds.; American Chemical Society: Washington, DC, 2006; Vol. 946, pp 103–116.
- (13) Rascón-Cruz, Q.; Sinagawa-García, S.; Osuna-Castro, J. A.; Bohorova, N.; Paredes-López, O. Accumulation, assembly, and digestibility of amaranthin expressed in transgenic tropical maize. *Theor. Appl. Genet.* **2004**, *108* (2), 335–342.
- (14) Tamas, C.; Kisgyorgy, B. N.; Rakszegi, M.; Wilkinson, M. D.; Yang, M. S.; Lang, L.; Tamas, L.; Bedo, Z. Transgenic approach to improve wheat (*Triticum aestivum* L.) nutritional quality. *Plant Cell Rep.* **2009**, *28* (7), 1085–1094.
- (15) Chakraborty, S.; Chakraborty, N.; Agrawal, L.; Ghosh, S.; Narula, K.; Shekhar, S.; Naik, P. S.; Pande, P. C.; Chakrborti, S. K.; Datta, A. Next-generation protein-rich potato expressing the seed protein gene AmA1 is a result of proteome rebalancing in transgenic tuber. *Proc. Natl. Acad. Sci. U.S.A.* **2010**, *107* (41), 17533–17538.
- (16) Huerta-Ocampo, J. A.; Barba de la Rosa, A. P. Amaranth: A pseudo-cereal with nutraceutical properties. *Curr. Nutr. Food Sci.* **2011**, *7*, 1–9.
- (17) Omami, E. N.; Hammes, P. S.; Robbertse, P. J. Differences in salinity tolerance for growth and water-use efficiency in some amaranth (*Amaranthus* spp.) genotypes. *N. Z. J. Crop Hortic. Sci.* **2006**, *34* (1), 11–22.
- (18) Delano-Frier, J. P.; Aviles-Arnaut, H.; Casarrubias-Castillo, K.; Casique-Arroyo, G.; Castrillon-Arbelaez, P. A.; Herrera-Estrella, L.; Massange-Sánchez, J.; Martínez-Gallardo, N. A.; Parra-Cota, F. I.; Vargas-Ortiz, E.; Estrada-Hernández, M. G. Transcriptomic analysis of grain amaranth (*Amaranthus hypochondriacus*) using 454 pyrosequencing: Comparison with *A. tuberculatus*, expression profiling in stems and in response to biotic and abiotic stress. *BMC Genomics* **2011**, *12*.
- (19) Huerta-Ocampo, J. A.; León-Galván, M. F.; Ortega-Cruz, L. B.; Barrera-Pacheco, A.; De León-Rodríguez, A.; Mendoza-Hernández, G.; Barba de la Rosa, A. P. Water stress induces up-regulation of DOF1 and MIF1 transcription factors and down-regulation of proteins involved in secondary metabolism in amaranth roots (*Amaranthus hypochondriacus* L.). *Plant Biol.* **2011**, *13* (3), 472–482.
- (20) Aguilar-Hernández, H. S.; Santos, L.; León-Galván, F.; Barrera-Pacheco, A.; Espitia-Rangel, E.; De León-Rodríguez, A.; Guevara-González, R. G.; Barba de la Rosa, A. P. Identification of calcium stress induced genes in amaranth leaves through suppression subtractive hybridization. *J. Plant Physiol.* **2011**, *168* (17), 2102–2109.
- (21) Lee, R. M.; Thimmapuram, J.; Thinglum, K. A.; Gong, G.; Hernandez, A. G.; Wright, C. L.; Kim, R. W.; Mikel, M. A.; Tranel, P. J. Sampling the Waterhemp (*Amaranthus tuberculatus*) Genome Using Pyrosequencing Technology. *Weed Sci.* **2009**, *57* (5), 463–469.
- (22) Magné, C.; Larher, F. High sugar content of extracts interferes with colorimetric determination of amino acids and free proline. *Anal. Biochem.* **1992**, *200* (1), 115–118.
- (23) Aghaei, K.; Ehsanpour, A. A.; Komatsu, S. Proteome Analysis of Potato under Salt Stress. *J. Proteome Res.* **2008**, *7* (11), 4858–4868.
- (24) Munns, R.; Tester, M. Mechanisms of salinity tolerance. In *Annu. Rev. Plant Biol.*; Annual Reviews: Palo Alto, 2008; Vol. 59, pp 651–681.
- (25) Maathuis, F. J. M. The role of monovalent cation transporters in plant responses to salinity. *J. Exp. Bot.* **2006**, *57* (5), 1137–1147.
- (26) Zhang, Z.; Mao, B.; Li, H.; Zhou, W.; Takeuchi, Y.; Yoneyama, K. Effect of salinity on physiological characteristics, yield and quality of microtubers in vitro in potato. *Acta Physiol. Plant.* **2005**, *27* (4), 481–489.
- (27) Yang, Y.; Thannhauser, T. W.; Li, L.; Zhang, S. Development of an integrated approach for evaluation of 2-D gel image analysis: Impact of multiple proteins in single spots on comparative proteomics in conventional 2-D gel/MALDI workflow. *Electrophoresis* **2007**, *28* (12), 2080–2094.
- (28) Leister, D. Chloroplast research in the genomic age. *Trends Genetics* **2003**, *19* (1), 47–56.
- (29) Emanuelsson, O.; Nielsen, H.; Brunak, S.; von Heijne, G. Predicting Subcellular Localization of Proteins Based on their N-terminal Amino Acid Sequence. *J. Mol. Biol.* **2000**, *300* (4), 1005–1016.
- (30) Kleffmann, T.; Hirsch-Hoffmann, M.; Gruisse, W.; Baginsky, S. plprot: A Comprehensive Proteome Database for Different Plastid Types. *Plant Cell Physiol.* **2006**, *47* (3), 432–436.
- (31) Wojtyla, L.; Kosmala, A.; Garncarska, M. Lupine embryo axes under salinity stress. II. Mitochondrial proteome response. *Acta Physiol. Plant.* **2013**, *35* (8), 2383–2392.
- (32) Chivasa, S.; Tomé, D. F. A.; Hamilton, J. M.; Slabas, A. R. Proteomic Analysis of Extracellular ATP-Regulated Proteins Identifies ATP Synthase β -Subunit as a Novel Plant Cell Death Regulator. *Mol. Cell. Proteomics* **2011**, *10*.1074/mcp.M110.003905
- (33) Taylor, N. L.; Heazlewood, J. L.; Day, D. A.; Millar, A. H. Differential impact of environmental stresses on the pea mitochondrial proteome. *Mol. Cell. Proteomics* **2005**, *4* (8), 1122–1133.
- (34) Chen, S.; Gollop, N.; Heuer, B. Proteomic analysis of salt-stressed tomato (*Solanum lycopersicum*) seedlings: effect of genotype and exogenous application of glycinebetaine. *J. Exp. Bot.* **2009**, *60* (7), 2005–2019.
- (35) Chen, X.; Wang, Y.; Li, J.; Jiang, A.; Cheng, Y.; Zhang, W. Mitochondrial proteome during salt stress-induced programmed cell death in rice. *Plant Physiol. Biochem.* **2009**, *47* (5), 407–415.
- (36) Suzuki, N.; Rizhsky, L.; Liang, H. J.; Shuman, J.; Shulaev, V.; Mittler, R. Enhanced tolerance to environmental stress in transgenic plants expressing the transcriptional coactivator multiprotein bridging factor 1c. *Plant Physiol.* **2005**, *139* (3), 1313–1322.
- (37) Du, C. X.; Fan, H. F.; Guo, S. R.; Tezuka, T.; Li, J. A. Proteomic analysis of cucumber seedling roots subjected to salt stress. *Phytochemistry* **2010**, *71* (13), 1450–1459.
- (38) Schaeffer, G. W.; Sharpe, F. T.; Sicher, R. C. Fructose 1,6-bisphosphate aldolase activity in leaves of a rice mutant selected for enhanced lysine. *Phytochemistry* **1997**, *46* (8), 1335–1338.
- (39) Yan, S. P.; Tang, Z. C.; Su, W.; Sun, W. N. Proteomic analysis of salt stress-responsive proteins in rice root. *Proteomics* **2005**, *5* (1), 235–244.
- (40) Sarhadi, E.; Bazargani, M. M.; Sajise, A. G.; Abdolah, S.; Vispo, N. A.; Arceta, M.; Nejad, G. M.; Singh, R. K.; Salekdeh, G. H. Proteomic analysis of rice anthers under salt stress. *Plant Physiol. Biochem.* **2012**, *58*, 280–287.
- (41) Kav, N. N. V.; Srivastava, S.; Goonewardene, L.; Blade, S. F. Proteome-level changes in the roots of *Pisum sativum* in response to salinity. *Ann. Appl. Biol.* **2004**, *145* (2), 217–230.
- (42) Ndimba, B. K.; Chivasa, S.; Simon, W. J.; Slabas, A. R. Identification of *Arabidopsis* salt and osmotic stress responsive proteins using two-dimensional difference gel electrophoresis and mass spectrometry. *Proteomics* **2005**, *5* (16), 4185–4196.
- (43) Gao, F.; Zhou, Y.; Huang, L.; He, D.; Zhang, G. Proteomic analysis of long-term salinity stress-responsive proteins in *Thellungiella halophila* leaves. *Chin. Sci. Bull.* **2008**, *53* (22), 3530–3537.
- (44) Rocco, M.; Lomaglio, T.; Loperte, A.; Satriani, A. Metapontum Forest Reserve: Salt Stress Responses in *Pinus halepensis*. *Am. J. Plant Sci.* **2013**, *4* (3), 674–684.
- (45) Galat, A. Peptidylprolyl cis/trans isomerases (immunophilins): biological diversity–targets–functions. *Curr. Top. Med. Chem.* **2003**, *3* (12), 1315–1347.
- (46) Chen, A. P.; Wang, G. L.; Qu, Z. L.; Lu, C. X.; Liu, N.; Wang, F.; Xia, G. X. Ectopic expression of ThCYP1, a stress-responsive

- cyclophilin gene from *Thellungiella halophila*, confers salt tolerance in fission yeast and tobacco cells. *Plant Cell Rep.* **2007**, *26* (2), 237–45.
- (47) Kumari, S.; Singh, P.; Singla-Pareek, S. L.; Pareek, A. Heterologous expression of a salinity and developmentally regulated rice cyclophilin gene (OsCyp2) in *E. coli* and *S. cerevisiae* confers tolerance towards multiple abiotic stresses. *Mol. Biotechnol.* **2009**, *42* (2), 195–204.
- (48) Zhu, C.; Wang, Y.; Li, Y.; Bhatti, K. H.; Tian, Y.; Wu, J. Overexpression of a cotton cyclophilin gene (GhCyp1) in transgenic tobacco plants confers dual tolerance to salt stress and *Pseudomonas syringae* pv. tabaci infection. *Plant Physiol. Biochem.* **2011**, *49* (11), 1264–1271.
- (49) Jia, X.-Y.; He, L.-H.; Jing, R.-L.; Li, R.-Z. Calreticulin: conserved protein and diverse functions in plants. *Physiol. Plant.* **2009**, *136* (2), 127–138.
- (50) Jiang, Y.; Yang, B.; Harris, N. S.; Deyholos, M. K. Comparative proteomic analysis of NaCl stress-responsive proteins in *Arabidopsis* roots. *J. Exp. Bot.* **2007**, *58* (13), 3591–3607.
- (51) Nam, M. H.; Huh, S. M.; Kim, K. M.; Park, W. J.; Seo, J. B.; Cho, K.; Kim, D. Y.; Kim, B. G.; Yoon, I. S. Comparative proteomic analysis of early salt stress-responsive proteins in roots of SnRK2 transgenic rice. *Proteome Sci.* **2012**, *10*.
- (52) Escobar Galvis, M. L.; Marttila, S.; Häkansson, G.; Forsberg, J.; Knorpp, C. Heat Stress Response in Pea Involves Interaction of Mitochondrial Nucleoside Diphosphate Kinase with a Novel 86-Kilodalton Protein. *Plant Physiol.* **2001**, *126* (1), 69–77.
- (53) Xiong, L.; Zhu, J. K. Molecular and genetic aspects of plant responses to osmotic stress. *Plant, Cell Environ.* **2002**, *25* (2), 131–139.
- (54) Shin, S. Y.; Kim, M. H.; Kim, Y. H.; Park, H. M.; Yoon, H. S. Co-expression of monodehydroascorbate reductase and dehydroascorbate reductase from *Brassica rapa* effectively confers tolerance to freezing-induced oxidative stress. *Mol. Cells* **2013**, *36* (4), 304–315.
- (55) Park, S. K.; Jung, Y. J.; Lee, J. R.; Lee, Y. M.; Jang, H. H.; Lee, S. S.; Park, J. H.; Kim, S. Y.; Moon, J. C.; Lee, S. Y.; Chae, H. B.; Shin, M. R.; Jung, J. H.; Kim, M. G.; Kim, W. Y.; Yun, D.-J.; Lee, K. O.; Lee, S. Y. Heat-Shock and Redox-Dependent Functional Switching of an h-Type *Arabidopsis* Thioredoxin from a Disulfide Reductase to a Molecular Chaperone. *Plant Physiol.* **2009**, *150* (2), 552–561.
- (56) Sun, L.; Ren, H.; Liu, R.; Li, B.; Wu, T.; Sun, F.; Liu, H.; Wang, X.; Dong, H. An h-Type Thioredoxin Functions in Tobacco Defense Responses to Two Species of Viruses and an Abiotic Oxidative Stress. *Mol. Plant-Microbe Interact.* **2010**, *23* (11), 1470–1485.
- (57) Zhang, L.; Tian, L.-H.; Zhao, J.-F.; Song, Y.; Zhang, C.-J.; Guo, Y. Identification of an Apoplastic Protein Involved in the Initial Phase of Salt Stress Response in Rice Root by Two-Dimensional Electrophoresis. *Plant Physiol.* **2009**, *149* (2), 916–928.
- (58) Zhang, C. J.; Zhao, B. C.; Ge, W. N.; Zhang, Y. F.; Song, Y.; Sun, D. Y.; Guo, Y. An apoplastic h-type thioredoxin is involved in the stress response through regulation of the apoplastic reactive oxygen species in rice. *Plant Physiol.* **2011**, *157* (4), 1884–99.
- (59) Kosova, K.; Prail, I. T.; Vitamvas, P. Protein contribution to plant salinity response and tolerance acquisition. *Int. J. Mol. Sci.* **2013**, *14* (4), 6757–6789.
- (60) Jung, T.; Höhn, A.; Grune, T. The proteasome and the degradation of oxidized proteins: Part III—Redox regulation of the proteasomal system. *Redox Biol.* **2014**, *2* (0), 388–394.
- (61) Kurepa, J.; Wang, S.; Li, Y.; Smalle, J. Proteasome regulation, plant growth and stress tolerance. *Plant Signaling Behav.* **2009**, *4* (10), 924–927.
- (62) Ozgur, R.; Uzilday, B.; Sekmen, A. H.; Turkan, I. Reactive oxygen species regulation and antioxidant defence in halophytes. *Funct. Plant Biol.* **2013**, *40* (9), 832–847.
- (63) Askari, H.; Edqvist, J.; Hajheidari, M.; Kafi, M.; Salekdeh, G. H. Effects of salinity levels on proteome of *Suaeda aegyptiaca* leaves. *Proteomics* **2006**, *6* (8), 2542–2554.
- (64) Wang, X.; Fan, P.; Song, H.; Chen, X.; Li, X.; Li, Y. Comparative Proteomic Analysis of Differentially Expressed Proteins in Shoots of *Salicornia europaea* under Different Salinity. *J. Proteome Res.* **2009**, *8* (7), 3331–3345.
- (65) Ramachandran, S.; Christensen, H. E. M.; Ishimaru, Y.; Dong, C. H.; Chao-Ming, W.; Cleary, A. L.; Chua, N. H. Profilin plays a role in cell elongation, cell shape maintenance, and flowering in *Arabidopsis*. *Plant Physiol.* **2000**, *124* (4), 1637–1647.
- (66) Wang, C.; Zhang, L. J.; Huang, R. D. Cytoskeleton and plant salt stress tolerance. *Plant Signaling Behav.* **2011**, *6* (1), 29–31.
- (67) Caruso, G.; Cavaliere, C.; Guarino, C.; Gubbotti, R.; Foglia, P.; Lagana, A. Identification of changes in *Triticum durum* L. leaf proteome in response to salt stress by two-dimensional electrophoresis and MALDI-TOF mass spectrometry. *Anal. Bioanal. Chem.* **2008**, *391* (1), 381–390.
- (68) Bandehagh, A.; Salekdeh, G. H.; Toorchi, M.; Mohammadi, A.; Komatsu, S. Comparative proteomic analysis of canola leaves under salinity stress. *PROTEOMICS* **2011**, *11* (10), 1965–1975.
- (69) Maleki, M.; Naghavi, M. R.; Alizadeh, H.; Poostini, K.; Abd Mishani, C. Comparison of Protein Changes in the Leaves of Two Bread Wheat Cultivars with Different Sensitivity under Salt Stress. *Annu. Rev. Biol.* **2014**, *4* (11), 1784–1797.
- (70) Sobhanian, H.; Razavizadeh, R.; Nanjo, Y.; Ehsanpour, A.; Jazii, F.; Motamed, N.; Komatsu, S. Proteome analysis of soybean leaves, hypocotyls and roots under salt stress. *Proteome Sci.* **2010**, *8* (1), 19.
- (71) Baisakh, N.; Subudhi, P.; Varadwaj, P. Primary responses to salt stress in a halophyte, smooth cordgrass (*Spartina alterniflora* Loisel.). *Funct. Integr. Genomics* **2008**, *8* (3), 287–300.
- (72) Hajheidari, M.; Abdollahian-Noghabi, M.; Askari, H.; Heidari, M.; Sadeghian, S. Y.; Ober, E. S.; Salekdeh, G. H. Proteome analysis of sugar beet leaves under drought stress. *Proteomics* **2005**, *5* (4), 950–960.
- (73) Parisi, G.; Perales, M.; Fornasari, M. S.; Colaneri, A.; Gonzalez-Schain, N.; Gomez-Casati, D.; Zimmermann, S.; Brennicke, A.; Araya, A.; Ferry, J. G.; Echave, J.; Zabaleta, E. Gamma carbonic anhydrases in plant mitochondria. *Plant Mol. Biol.* **2004**, *55* (2), 193–207.
- (74) Yu, S.; Zhang, X. X.; Guan, Q. J.; Takano, T.; Liu, S. K. Expression of a carbonic anhydrase gene is induced by environmental stresses in rice (*Oryza sativa* L.). *Biotechnol. Lett.* **2007**, *29* (1), 89–94.
- (75) Yoo, K. S.; Ok, S. H.; Jeong, B.-C.; Jung, K. W.; Cui, M. H.; Hyoung, S.; Lee, M.-R.; Song, H. K.; Shin, J. S. Single Cystathione β -Synthase Domain-Containing Proteins Modulate Development by Regulating the Thioredoxin System in *Arabidopsis*. *Plant Cell Online* **2011**, *23* (10), 3577–3594.
- (76) Singh, A.; Kumar, R.; Pareek, A.; Sopory, S.; Singla-Pareek, S. Overexpression of Rice CBS Domain Containing Protein Improves Salinity, Oxidative, and Heavy Metal Tolerance in Transgenic Tobacco. *Molecular Biotechnology* **2012**, *52* (3), 205–216.
- (77) Délano-Frier, J. P.; Martínez-Gallardo, N. A. The transcriptome of *Amaranthus hypochondriacus* L.: A powerful tool for its deeper understanding and utilization. In *Amaranto: Ciencia y Tecnología. Libro Científico No. 2*, Primera Edición; Espitia-Rangel, E., Ed.; INIFAP/SINAREFI: México, 2012; pp 31–48.
- (78) Navarro-Meléndez, A.; Valdés-Rodríguez, S. E.; Délano-Frier, J. P. Proteomic analysis of amaranth subjected to herbivory and elicitors of insect resistance. In *Amaranto: Ciencia y Tecnología. Libro Científico No. 2*, Primera Edición; Espitia-Rangel, E., Ed.; INIFAP/SINAREFI: México, 2012; pp 75–84.
- (79) Heath, R. J.; Rock, C. O. Roles of the FabA and FabZ beta-hydroxyacyl-acyl carrier protein dehydratases in *Escherichia coli* fatty acid biosynthesis. *J. Biol. Chem.* **1996**, *271* (44), 27795–27801.
- (80) Zhou, S. P.; Sauve, R.; Thannhauser, T. W. Proteome changes induced by aluminium stress in tomato roots. *J. Exp. Bot.* **2009**, *60* (6), 1849–1857.
- (81) Li, D.; Su, Z.; Dong, J.; Wang, T. An expression database for roots of the model legume *Medicago truncatula* under salt stress. *BMC Genomics* **2009**, *10*, 517.
- (82) Klinke, S.; Zylberman, V.; Bonomi, H. R.; Haase, I.; Guimarães, B. G.; Braden, B. C.; Bacher, A.; Fischer, M.; Goldbaum, F. A. Structural and Kinetic Properties of Lumazine Synthase Isoenzymes in the Order Rhizobiales. *J. Mol. Biol.* **2007**, *373* (3), 664–680.

- (83) Xiao, S.; Dai, L.; Liu, F.; Wang, Z.; Peng, W.; Xie, D. COS1: An Arabidopsis coronatine insensitive1 Suppressor Essential for Regulation of Jasmonate-Mediated Plant Defense and Senescence. *Plant Cell Online* **2004**, *16* (5), 1132–1142.
- (84) Takeuchi, K.; Gyohda, A.; Tominaga, M.; Kawakatsu, M.; Hatakeyama, A.; Ishii, N.; Shimaya, K.; Nishimura, T.; Riemann, M.; Nick, P.; Hashimoto, M.; Komano, T.; Endo, A.; Okamoto, T.; Jikumaru, Y.; Kamiya, Y.; Terakawa, T.; Koshiba, T. RSOsPR10 expression in response to environmental stresses is regulated antagonistically by jasmonate/ethylene and salicylic acid signaling pathways in rice roots. *Plant Cell Physiol.* **2011**, *52* (9), 1686–1696.
- (85) Jain, S.; Srivastava, S.; Sarin, N. B.; Kav, N. N. V. Proteomics reveals elevated levels of PR 10 proteins in saline-tolerant peanut (*Arachis hypogaea*) calli. *Plant Physiol. Biochem.* **2006**, *44* (4), 253–259.
- (86) Sugimoto, M.; Takeda, K. Proteomic Analysis of Specific Proteins in the Root of Salt-Tolerant Barley. *Biosci., Biotechnol., Biochem.* **2009**, *73* (12), 2762–2765.
- (87) Marchler-Bauer, A.; Zheng, C. J.; Chitsaz, F.; Derbyshire, M. K.; Geer, L. Y.; Geer, R. C.; Gonzales, N. R.; Gwadz, M.; Hurwitz, D. I.; Lanczycki, C. J.; Lu, F.; Lu, S. N.; Marchler, G. H.; Song, J. S.; Thanki, N.; Yamashita, R. A.; Zhang, D. C.; Bryant, S. H. CDD: conserved domains and protein three-dimensional structure. *Nucleic Acids Res.* **2013**, *41* (D1), D348–D352.
- (88) Chen, J.-Y.; Dai, X.-F. Cloning and characterization of the *Gossypium hirsutum* major latex protein gene and functional analysis in *Arabidopsis thaliana*. *Planta* **2010**, *231* (4), 861–873.
- (89) Peumans, W. J.; Hause, B.; Van Damme, E. J. M. The galactose-binding and mannose-binding jacalin-related lectins are located in different sub-cellular compartments. *FEBS Lett.* **2000**, *477* (3), 186–192.
- (90) Chitteti, B. R.; Peng, Z. Proteome and Phosphoproteome Differential Expression under Salinity Stress in Rice (*Oryza sativa*) Roots. *J. Proteome Res.* **2007**, *6* (5), 1718–1727.
- (91) Aghaei, K.; Ehsanpour, A.; Shah, A.; Komatsu, S. Proteome analysis of soybean hypocotyl and root under salt stress. *Amino Acids* **2009**, *36* (1), 91–98.
- (92) Xiang, Y.; Song, M.; Wei, Z.; Tong, J.; Zhang, L.; Xiao, L.; Ma, Z.; Wang, Y. A jacalin-related lectin-like gene in wheat is a component of the plant defence system. *J. Exp. Bot.* **2011**, *62*, 5471–5483.
- (93) Witzel, K.; Matros, A.; Strickert, M.; Kaspar, S.; Peukert, M.; Mühlung, K. H.; Börner, A.; Mock, H.-P. Salinity Stress in Roots of Contrasting Barley Genotypes Reveals Time-Distinct and Genotype-Specific Patterns for Defined Proteins. *Mol. Plant* **2014**, *7* (2), 336–355.
- (94) Qian, D.; Jiang, L.; Lu, L.; Wei, C.; Li, Y. Biochemical and structural properties of cyanases from *Arabidopsis thaliana* and *Oryza sativa*. *PLoS One* **2011**, *6* (3), e18300 DOI: 10.1371/journal.pone.0018300.
- (95) Li, Y.; Cohenford, M.; Dutta, U.; Dain, J. The structural modification of DNA nucleosides by nonenzymatic glycation: an in vitro study based on the reactions of glyoxal and methylglyoxal with 2'-deoxyguanosine. *Anal. Bioanal. Chem.* **2008**, *390* (2), 679–688.
- (96) Yadav, S. K.; Singla-Pareek, S. L.; Ray, M.; Reddy, M. K.; Sopory, S. K. Methylglyoxal levels in plants under salinity stress are dependent on glyoxalase I and glutathione. *Biochem. Biophys. Res. Commun.* **2005**, *337* (1), 61–67.
- (97) Wu, C.; Ma, C.; Pan, Y.; Gong, S.; Zhao, C.; Chen, S.; Li, H. Sugar beet M14 glyoxalase I gene can enhance plant tolerance to abiotic stresses. *J. Plant Res.* **2013**, *126* (3), 415–425.